GeoScienceWorld
Lithosphere
Volume 2020, Article ID 8861007, 20 pages
https://doi.org/10.2113/2020/8861007

Lithosphere

Research Article

Seismic Evidence for Proterozoic Collisional Episodes along Two Geosutures within the Southern Granulite Province of India

Raju Prathigadapa,[1] **Subrata Das Sharma**,[1] **and Durbha Sai Ramesh**[2]

[1]*CSIR-National Geophysical Research Institute, Uppal Road, Hyderabad 500007, India*
[2]*Indian Institute of Geomagnetism, Colaba, Mumbai 400005, India*

Correspondence should be addressed to Raju Prathigadapa; paraju@ngri.res.in

Received 26 September 2019; Accepted 18 August 2020; Published 15 October 2020

Academic Editor: Sarah Roeske

The Southern Granulite Province of India had witnessed episodes of multiple tectonic activities, leading to sparsely preserved surface geological features. The present study is focused on unraveling the geodynamic evolution of this terrain through measurement of Moho depth and Vp/Vs ratio using data from a large number of broadband seismic stations. These results unambiguously establish three domains distinct in Moho depth and crustal composition. An intermediate to felsic crust with a 7–10 km step-in-Moho is delineated across the Moyar–Bhavani region. Anomalously high felsic crust with abrupt jump in Moho (~8–10 km) together with a dipping feature at deeper level characterizes the transition from eastern to southern segments of the Jhavadi–Kambam–Trichur region. By contrast, the central zone hosting the Palghat–Cauvery shear zone records uniform felsic crust and flat Moho. Drawing analogy from similar results in different parts of the globe, juxtaposition of petrologically dissimilar crustal blocks characterized by varied depths to the Moho is argued to point towards unambiguous presence of two distinct geosutures in the study area: one along the Moyar–Bhavani region and the other across the Jhavadi–Kambam–Trichur. This inference is corroborated by the presence of layered meta-anorthosite, related rock suites, and mafic-ultramafic bodies, supporting the view of a suprasubduction setting in the Moyar–Bhavani region. The Jhavadi–Kambam–Trichur area is marked by operation of the Wilson cycle by way of sparsely preserved geological features such as the presence of *ophirags* (ophiolite fragments), alkali syenites, and carbonatites. Geochronological results suggest that the suturing along Moyar–Bhavani took place during the Paleoproterozoic and that along Jhavadi–Kambam–Trichur was during the late Neoproterozoic.

1. Introduction

The Archean Dharwar Craton represents an inclined cross-section of the crust in southern India such that the greenschist facies rocks are exposed on the surface towards north, amphibolite facies in the middle, and granulite facies rocks to the south [1, 2]. The transition from amphibolite to granulite facies is marked by occurrences of (i) pseudo charnockites that resemble charnockites in terms of greasy appearance but devoid of hypersthenes and are actually diopsidic gneisses [3], (ii) incipient or arrested charnockite patches, and (iii) basic granulite dykes with plagioclase clouding [4]. Figure 1(a) shows the generalized geological map of the region (after [5]). The transition boundary from amphibolite to granulite facies is popularly known as the "Fermor line" ([6]; see Figure 1(a)). The south of this transition boundary forms the Southern Granulite Province (SGP). Two major aspects of the Southern Granulite Province that are central and have attracted the attention of geoscientists from across the world are (i) to provide a suitable model for the genesis of granulite facies rocks [7–9] and (ii) to understand the role played by the Southern Granulite Province during the amalgamation and break-up of the Gondwanaland [10–12]. Numerous studies encompassing a wide variety of tools that include geological, geochemical, geophysical, and geochronological studies were therefore conducted by many researchers from different countries to understand the genesis and evolution of this province (e.g., [12–21]; [11, 22–27]). Based on some of the significant studies, it is now broadly understood that the

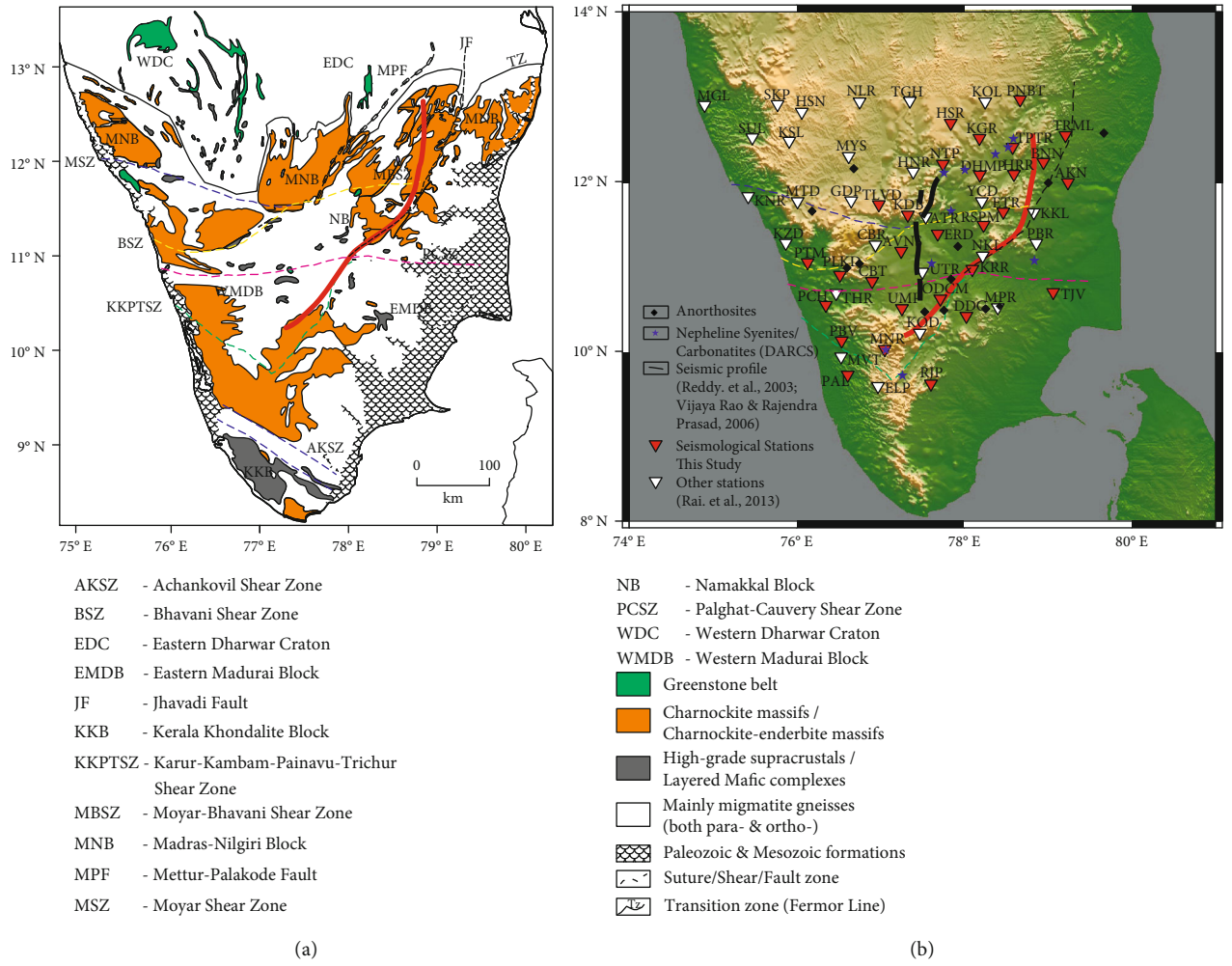

FIGURE 1: Map of the Southern Granulite Province of India. (a) Generalized geological map of the region (after [5]). To the south of Archean Dharwar Craton, rocks are metamorphosed to granulite facies [6]. This transition from amphibolite to granulite facies is popularly known as the "Fermor line" and is marked TZ (transition zone) in the figure. Major shear/fault zones (after [41]) are demarcated using diverse-colored broken lines. Thick red line represents a geosuture (after Das Sharma et al. [28]). Various crustal blocks are after Ramakrishnan [4] and Brandt et al. [22]. (b) Location of broadband seismic stations. Red inverted triangles represent stations sited during the course of this work. White inverted triangles are stations (see Appendix) reported by Rai et al. [45]. The distribution of alkaline rocks and carbonatites (star) and anorthosites (diamonds) is shown. Suture/shear/fault zones are same as in (a). Thick black line represents seismic profile along the Kolattur–Palani transect [20, 64].

Gondwana assembly is characterized by late Neoproterozoic collisional orogeny and deformation marked by operation of Wilson cycle during the geological past. However, the location of the geosuture/geosutures within the high-grade rocks of southern India is highly controversial and debatable [4, 11, 13, 22, 24–26]. This is because the province is punctuated by several crustal-scale megashear zones (Figure 1) such as the Moyar shear zone (MSZ) and the Bhavani shear zone (BSZ) together forming the Moyar–Bhavani shear zone (MBSZ), the Palghat–Cauvery shear zone (PCSZ), the Karur–Kambam–Painavu–Trichur shear zone (KKPTSZ), and the Achankovil shear zone (AKSZ). Evidently, these shear zones form the key tectonic elements of the Southern Granulite Province. However, the nature and evolution of these megashear zones of the Southern Granulite Province, viz., MBSZ, PCSZ, and KKPTSZ, are ambiguous in the absence of information related primarily to their depth disposition. In other words, the basic question related to disposition of suture(s) in three dimensions with their location needs to be addressed and established unambiguously.

In a recent study, the crustal structure beneath a prominent and crucial segment of the Southern Granulite Province using passive seismological experiment was investigated by us (Das Sharma et al. [28]). Based on the *Ps* receiver function analyses and H-κ stacking [29] results, it was demonstrated that the seismic structures of the crust across the Jhavadi–Karur–Kambam region within the Southern Granulite Province are distinct. Their dissimilar nature is manifested in terms of differences in the estimated average crustal compositions (Vp/Vs ratios) and Moho depths across this boundary. Our seismological results, when integrated with available geochronological data and preserved geological features such as presence of *ophirags* (ophiolite fragments)

and occurrence of alkali syenites and carbonatites in the area, could establish unambiguous presence of a geosuture along the Jhavadi–Karur–Kambam region.

Subsequent to these interesting seismological results (across the Jhavadi–Karur–Kambam region), a more detailed investigation was undertaken over a wide area of the Southern Granulite Province through installation of broadband seismic stations in a phased manner at other locations (total 29 stations; see Figure 1(b)). It is pertinent to mention that while data from mere 15 stations focusing on the Jhavadi–Karur–Kambam segment were published earlier by us (Das Sharma et al. [28]), the present research study is based on data from twice the number of stations, covering all the three major shear zones of Southern Granulite Province, viz., the Jhavadi–Karur–Kambam–Trichur shear zone (JKKTSZ), the Palghat–Cauvery shear zone (PCSZ), and the Moyar–Bhavani shear zone (MBSZ). The objectives of this study are therefore more rigorous and broad. Our aim is to evaluate the average seismological character (Moho depth and Vp/Vs ratio) of the crust across three major shear zones, viz., the Jhavadi–Karur–Kambam–Trichur shear zone (JKKTSZ), the Palghat–Cauvery shear zone (PCSZ), and the Moyar–Bhavani shear zone (MBSZ) through *Ps* receiver function analyses such as the H-κ stacking method. We also present CCP stack sections along select profiles, to confirm step-in-depth to Moho across JKKTSZ, besides observation of a dipping feature at some stations, reinforcing our earlier inference about the presence of a suture across this boundary. The CCP stacks also cover two other prominent shear zones of Southern Granulite Province, viz., PCSZ and MBSZ. Together, these effectively offered unprecedented insights into the character, status, and evolution of all the megashear zones of the region in a comprehensive manner from the perspective of operation of the Wilson cycle in the Southern Granulite Province that were widely separated in space and time. Further, since the ratio of compressional to shear wave velocity of crustal rocks depends on the nature of the crust (i e., Vp/Vs ratio depends on the average wt% SiO_2 of the crust; [30, 31]), the Vp/Vs ratio obtained from the H-κ stacking method is transformed to average wt% SiO_2 using a modified linear relationship between Vp/Vs and wt% SiO_2. The method for the estimation of average SiO_2 content from the Vp/Vs ratio is detailed in a subsequent section. The ultimate goal of this study is to evaluate the disposition and average compositional variation of the crust in three dimensions across the above-mentioned megashear zones based on seismological imaging. Such an attempt over the entire Southern Granulite Province of India is first of its kind and expected to yield a clear understanding about the role played by these megashear zones during geodynamic evolution of the Southern Granulite Province of India. This would eventually help to establish firmly the correlation of Southern Granulite Province of India with other segments of eastern Gondwana, when similar results in those segments accrue. Further, we also address some of the major concerns raised in the literature [4, 18, 32] pertaining to the V-shaped pattern of KKPTSZ (see Figure 1) mapped by Ghosh et al. [13]. Whether the KKPTSZ should be considered a terrane boundary was questioned by Ramakrishnan [4, 18] as well as Cenki and Kriegsman [32].

2. Geological Framework of the Study Area

The Southern Granulite Province of India, with an areal extent of ~40,000 km^2, is the third largest Precambrian granulite province of the world after Canada and Australia [33–35]. The "Fermor line" shown in Figure 1(a) represents the transition boundary across which metamorphism of rocks from amphibolite to granulite facies took place. The region south of the "Fermor line" represents the Southern Granulite Province of India. The granulite facies rocks (Figure 1(a)) occurring between the "Fermor line" and the E-W trending Moyar–Bhavani shear zone constitute the "Dharwar granulite belt" [4]. Drury et al. [36] were the first to propose a subdivision of the South Indian Shield into the Northern block and the Southern block, with the Palghat–Cauvery shear zone representing the tectonic boundary between them. In this subdivision, granulites of the Madras–Nilgiri block (Figure 1(a)) are included in the Northern block, whereas granulites occurring south of the Palghat–Cauvery shear zone constitute the Southern block. Subsequent to the subdivision proposed by Drury et al. [36], many researchers have used individual preferences to name different blocks of the South Indian Shield, leading to confusion among the readers. However, it is claimed by Ramakrishnan [4] that presently a consensus is arrived at regarding the usage of nomenclature of various blocks. According to this, the Southern Granulite Province is divided into four major blocks (e.g., [4]; see Figure 1), viz., the (1) Madras–Nilgiri block between the Fermor line and the Moyar–Bhavani shear zone, (2) Namakkal block lying between the Moyar–Bhavani shear zone and the Palghat–Cauvery shear zone, (3) Madurai block between the Palghat–Cauvery shear zone and the Achankovil shear zone, and (4) Kerala Khondalite block (also called the Trivandrum block), lying south of the Achankovil shear zone. Based on recent geochronological and geochemical studies, the Madurai block is further subdivided into western and eastern domains [22]. Likewise, the Kerala Khondalite block is also subdivided (not shown in Figure 1) into the northern Ponmudi block and the southern Nagercoil block [4].

The lithological association that is documented within the four major blocks of Southern Granulite Province is elaborated in detail by Ramakrishnan [4]. The granulites of the Namakkal block are products of 2.5 Ga metamorphic event with P-T-t path showing decompression of ~3 kbar during the Neoproterozoic [37]. The northern Dharwar granulite belt and the Namakkal as well as Madurai blocks include numerous alkali syenite plutons and anorthosites (Figure 1(b)). Massif-type anorthosite bodies within Madurai block are documented at various places such as Oddanchatram, Kadavur, and Perinthatta [38]. Besides these, occurrences of a number of anorogenic igneous intrusive bodies including pink granites are also documented. Although the igneous emplacement ages are of Neoproterozoic times (~0.8 Ga), the granitic protoliths show evidences of incorporation of older crustal components. For example, while the detrital zircons are as old as ~3 Ga, the younger granites

Table 1: Nature of crust (Moho depth and Vp/Vs ratio) of the Southern Granulite Province of India.

Station	Installation phase	Latitude (° N)	Longitude (° E)	Altitude (m)	Period of operation		No of RF	Moho depth (km)	Vp/Vs
					Start	End			
AKN	II	12.00	79.24	121	Jan 13	Feb 17	156	32.0 ± 0.13	1.68 ± 0.004
AVNS	IV	11.19	77.25	352	Feb 15	Feb17	66	44.6 ± 0.14	1.79 ± 0.006
BNN	II	12.24	78.95	212	Jan 13	Feb 17	168	30.6 ± 0.32	1.61 ± 0.006
CBT	I	10.84	76.90	247	Jun 11	Jan 15	131	42.9 ± 0.19	1.74 ± 0.004
DDG	I	10.43	78.02	252	Feb 11	Aug 12	204	42.9 ± 0.20	1.67 ± 0.005
DHMP	IV	12.09	78.18	490	Jan 15	Feb 17	68	43.1 ± 0.66	1.73 ± 0.021
ERD	I	11.40	77.68	196	Jun 11	May 15	301	43.7 ± 0.16	1.74 ± 0.006
ETR	II	11.66	78.46	292	Jan 13	Feb 17	182	46.6 ± 0.49	1.70 ± 0.010
HRR	I	12.10	78.59	337	Feb 11	May 15	438	43.6 ± 0.27	1.73 ± 0.011
HSR	I	12.70	77.84	860	Feb 11	Oct 12	141	31.9 ± 0.46	1.73 ± 0.017
KDB	III	11.62	77.33	825	Oct 14	Feb 17	84	45.4 ± 0.28	1.72 ± 0.006
KGR	II	12.52	78.18	494	Jan 13	Feb 17	144	33.4 ± 0.43	1.80 ± 0.009
KRR	II	10.98	78.09	130	Jan 13	Jan 15	151	42.4 ± 0.55	1.73 ± 0.017
MNR	I	10.04	77.05	1102	Feb 11	Feb 16	221	40.0 ± 0.24	1.72 ± 0.005
NTP	III	12.22	77.74	519	Oct 14	Feb 17	137	43.8 ± 0.36	1.71 ± 0.007
ODCM	IV	10.63	77.71	324	Jun 15	Feb 17	69	30.1 ± 0.69	1.72 ± 0.021
PAL	I	09.73	76.61	59	Feb 11	Apr 15	289	36.4 ± 0.44	1.75 ± 0.013
PCH		10.53	76.35	86	Jan 11	Dec 12	222	38.5 ± 0.11	1.77 ± 0.005
PBV	II	10.14	76.54	41	Jan 13	Feb 17	240	37.5 ± 0.69	1.75 ± 0.011
PLKD	IV	10.91	76.52	112	Feb 15	Feb 17	93	41.2 ± 0.46	1.75 ± 0.028
PNBT	IV	12.97	78.67	409	Feb 15	Feb 17	107	32.3 ± 0.14	1.73 ± 0.003
PTM	I	11.06	76.13	64	Feb 11	Jan 16	384	42.0 ± 0.14	1.74 ± 0.005
RJP	I	09.63	77.60	196	Jul 11	May 15	302	38.1 ± 0.27	1.76 ± 0.004
RSPM	IV	11.50	78.23	290	May 15	Feb 17	5	45.0 ± 0.77	1.72 ± 0.015
TJV	II	10.71	79.06	97	Jan 13	Jan 15	95	48.7 ± 0.44	1.71 ± 0.018
TLVD	IV	11.74	76.98	821	Oct 15	Sep 16	55	48.1 ± 0.49	1.73 ± 0.010
TPTR	IV	12.42	78.58	391	Feb 15	Feb 17	158	49.0 ± 0.14	1.68 ± 0.008
TRML	IV	12.55	79.21	169	Jun 15	Feb 17	85	33.0 ± 0.60	1.72 ± 0.023
UMP	I	10.52	77.26	374	Feb 11	Jan 15	302	41.4 ± 0.49	1.74 ± 0.028

indicate that they were emplaced at ~0.8–0.6 Ga [13, 22, 39–41]. The P-T-t studies conducted on sapphirine granulites in the Madurai block suggest that ultrahigh-temperature (840–1070°C) metamorphism with pressure ranging from 8.5 to 9.6 kbar and multistage exhumation history are characteristic of this area [42–44].

3. Data and Methods

The network of broadband seismic stations that was installed in the Southern Granulite Province of India for this study is of semipermanent nature. Installation of seismic stations at various locations was carried out in four separate time windows. Among the first group, ten broadband instruments were installed during 2011 (Table 1). However, two stations (DDG and HSR in Figure 1(b); see also Table 1) were discontinued in 2012 due to unforeseen problems, while the rest continued to operate. Seven more stations were sited during early 2013. Out of these seven stations, five seismometers were freshly acquired while two seismometers from DDG and HSR of the first phase were shifted to new locations. In the third phase, two more new stations became operational during 2014 (see Table 1). During the last phase, one new station (DHMP) was installed during January, 2015. Further, eight stations were relocated to new sites by shifting six seismometers of the first phase and two from the second phase. This was done during 2015. Seismological data from these 28 stations and a permanent broadband station PCH operated by CSIR-NGRI are processed and utilized in this study. These station locations (red inverted triangles) are shown in Figure 1(b). Data from 29 stations sited in this study are supplemented by similar published data from 26 other stations

located within the Southern Granulite Province and Dharwar Craton (see Appendix after [45]). In Figure 1(b), white inverted triangles represent the station locations reported by Rai et al. [45]. Thus, data pertaining to a total of 55 stations are utilized in this study during interpretation of the results. Five stations reported by Rai et al. [45], which fall in distinctly different lithological association constituting the Kerala Khondalite belt (viz., MVK, NGC, TKS, TRB, and TYD; not shown in Figure 1(b)), were not considered in our analysis.

3.1. Receiver Function Computation. It is well known that large velocity contrast across a discontinuity (e.g., Moho, 410 km or 660 km) causes a part of the steeply incident teleseismic P wave to convert into an SV wave. Besides the direct *P*-to-*s* (*Ps*) conversions, there are also many multiple reflections and conversions that occur between the surface and the interface (e.g., Moho). While the P wave and its multiples dominate the vertical component, *Ps*-converted waves and their multiples are prominently registered on the horizontal component (SV). Therefore, an appropriate component rotation into ray coordinate system isolates the *Ps* energy from that of P. The effects related to source, mantle propagation and instrument response, are suppressed by deconvolving the P waveform from the SV component, to obtain what are called receiver functions. The crustal multiples, designated as *Pps* and *Pss*, together with the direct conversion from the Moho boundary (*Pms*), contain a wealth of information concerning the average crustal properties such as the Moho thickness (H) and Vp/Vs value (related to Poisson's ratio, σ) in a well-constrained manner. Therefore, these useful parameters were evaluated and utilized in this study.

Teleseismic events with magnitudes greater than 5.5 Mb and epicentral distance range 30°–90° were used. The network of 29 stations recorded a total of 14582 events. Seismograms, with clear P wave registrations, recorded at each station, were selected for the receiver function analysis. A high-pass filter with corner frequency of 0.02 Hz was applied to the data. Radial and tangential components were obtained by rotating the horizontal components of the seismogram using corresponding back-azimuths. Receiver functions were computed using the radial and vertical components by applying a time-domain iterative deconvolution procedure [46]. To obtain better resolution of crustal layers, a Gaussian filter of width 2 was chosen during the iterative deconvolution. Thereafter, these receiver functions were visually inspected, and any conspicuously bad receiver functions were discarded. The number of receiver functions used for each station in final analysis are listed in Table 1. Such a processing procedure renders easy comparison of our receiver functions with the published data of Rai et al. [45].

3.2. Crustal Parameter Estimation by H-κ Stacking. Zhu and Kanamori [29] proposed a grid search method for the estimation of the Vp/Vs ratio (κ) and the crustal thickness (H). In this method, the weighted amplitudes of the converted waves at the Moho and corresponding multiples in crust recorded on radial receiver functions are stacked at their respective predicted arrival times using the standard IASP91 velocity model.

Assuming a homogeneous P wave velocity in the crust, we therefore applied the stacking technique which sums the receiver function amplitudes at the predicted arrival times of the crustal phases, *Pms*, *Pps*, and *Pss*, for a combination of crustal thickness (H) and Vp/Vs (κ) values. The values of H and κ for which all the three phases stack coherently and the sum reaches a maximum value were taken to be the estimates of the crustal thickness and Vp/Vs. In the present study, a Vp of 6.3 km/s was used and a grid search was performed over the H and κ ranges of 20 to 60 km and 1.5 to 2.0, respectively. The average crustal Vp/Vs ratio is a measure of crustal elastic property. It is related to Poisson's ratio in accordance with the following equation:

$$\frac{Vp}{Vs} = \sqrt{\frac{2(\sigma - 1)}{(2\sigma - 1)}}, \tag{1}$$

$$\text{or } \sigma = \frac{\left[(Vp/Vs)^2 - 2\right]}{2\left[(Vp/Vs)^2 - 1\right]}. \tag{2}$$

The advantage of the Zhu and Kanamori [29] method is that it excludes the need to pick the arrival times of seismic phases. Therefore, large amounts of teleseismic waveforms can be processed easily. By stacking receiver functions from various azimuths and distances, one gets the average structure of the crust where the effects of lateral structure variation are suppressed [29].

3.3. Common Conversion Point (CCP) Binning. In order to get adequate insight into the nature of the underlying crust in the study area, we also carried out 2D common conversion point (CCP) stacking at certain critical segments using the FuncLab toolbox [47, 48]. The toolbox implements the CCP stacking method of Dueker and Sheehan [49]. Receiver functions from 29 stations totaling to ~3000 were handpicked by visual examination of the computed receiver functions. All these selected receiver functions display clear Moho arrivals and a good signal-to-noise ratio.

The receiver functions from all the stations were transformed into the depth domain by back-projecting the energy to their corresponding conversion points along their paths at every 1 km, using the IASP91 standard velocity model. To enhance the spatial coherence of the converted phases, these amplitudes corresponding to different depth-offsets are subsequently projected onto a 2D reference plane. The optimal choice of this plane is based on the subsurface geometry, station disposition, and pierce point distribution. The back-projected amplitudes of the RFs falling in a spatial grid are stacked using move-out corrections and plotted using a color scheme where red represents a positive polarity and blue indicates a negative one. In this study, we used a grid size of 0.5 × 3 sq. km in the depth range 0–100 km to obtain a relatively high-resolution image for each selected profile. Such depth-migrated receiver functions produce 2D CCP stack cross-sections.

3.4. Estimation of Average SiO_2 Content from the Vp/Vs Ratio. Using pulse transmission technique, Christensen and Mooney [31] and Christensen [30] measured the compressional (Vp) and shear (Vs) wave velocity of mineral and rock samples that essentially comprise the important constituents of the crust globally. Then, the Poisson ratio (σ) was calculated using the standard relation shown in equation (1). As a second step in the analyses, the wt% SiO_2 in each sample was determined. Finally, a relationship between the wt% SiO_2 and Poisson's ratio σ was arrived at (see Table 3 and Figure 13 of [30]). Based on the results, it was pointed out by Christensen [30] that there exists a good agreement between the experimentally determined Poisson's ratios of monomineralic rocks and those calculated from single-crystal elastic constants. For igneous and metamorphic rocks, he observed that Poisson's ratios correlate qualitatively with mineralogical changes. The overall trend is nonlinear [30] in the binary plot between weight percent SiO_2 and Poisson's ratio (σ). However, σ increases with decreasing SiO_2 content and exhibits a linear correlation between 55 and 75 wt% SiO_2. Based on such an analysis, Christensen [30] proposed that measurements of Poisson's ratio might provide valuable information on average crustal chemistry of a region. The validity of the relationship proposed by Christensen [30] was subsequently verified by a large number of workers covering diverse geological terrains having variable antiquity (e.g., [50–53]).

The relationship between wt% SiO_2 and Poisson's ratio (σ) obtained by Christensen [30] was reevaluated by us (see also [28]). We used the data given in Christensen [30] for 18 different rock types of metasedimentary and igneous origins that essentially comprise the important constituents of crustal geology. These include quartzite, slate, metagraywacke, paragranulite, felsic and mafic granulites, granite, basalt, diorite, and anorthosite. We then explored the relationship between Vp/Vs and SiO_2. This exercise yielded an excellent linear relationship between Vp/Vs and SiO_2 (with $R^2 = 0.88$) for the entire compositional range of the crust (Figure 2). Such a good correlation is in concert with the documented decrease in compressional wave velocities with concomitant increase in shear wave velocities as a function of SiO_2 content [30]. The estimated linear relation (Figure 2) is used to compute the average crustal wt% SiO_2 using the Vp/Vs ratio obtained from the H-κ stacking method beneath each station shown in Figure 1(b).

It is therefore important to note that the SiO_2 values presented as a linear function of Vp/Vs (Figure 2) could represent a general case for average crust globally. The SiO_2 content obtained in this study using the measured Vp/Vs values (from the H-κ stacking method) correspond to the study area, i.e., the Southern Granulite Province of India.

4. Results and Discussion

The results pertaining to 29 stations that were sited within the Southern Granulite Province of India for the present study are presented in Table 1. The measured parameters include the average crustal depth (Moho) and Vp/Vs ratio pertaining to each independent broadband seismic station. Standard bootstrap technique (see [28]) was used to estimate the uncertainty in the H and Vp/Vs values.

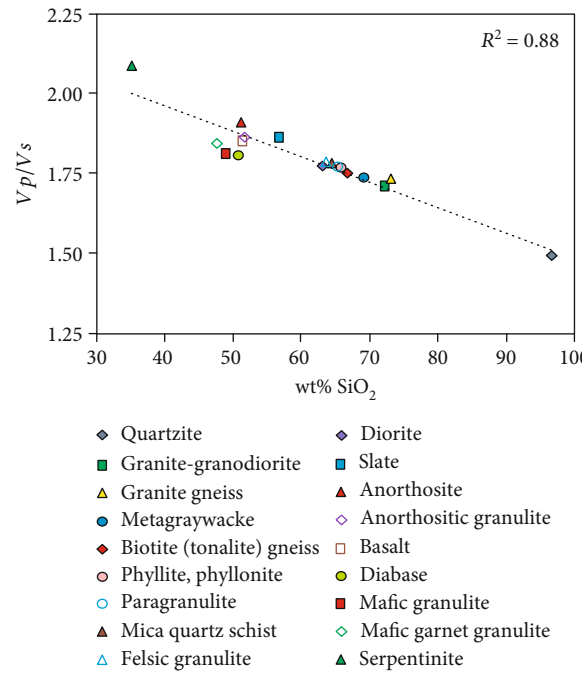

Figure 2: Relationship between average SiO_2 content and corresponding Vp/Vs ratio. All common crustal rock types are shown in the diagram (data from [30]). Excellent linear correlation ($R^2 = 0.88$) can be observed between the plotted parameters. This diagram forms the basis for estimation of average crustal SiO_2 content of the study area and is presented in Figure 8(b) using Vp/Vs ratios recorded at various stations.

4.1. Observations from the Receiver Function Stack Sections and H-κ Stacking Results. Figure 3 presents *Ps* receiver function distance stack sections from the study region corresponding to representative broadband seismic stations plotted against the back-azimuth (BAZ) of each event. The first positive arrival on each trace at time zero is the direct P arrival, and the next highest positive amplitude arrival is the *P*-to-*s*-converted wave signal from the Moho (*Pms*). A major observation from Figure 3 is that the sum traces record large variations in the delay times of the *Pms* arrival. The Moho depth varies from 30.1 to 49.0 km (Table 1). Similar large variations (see Appendix) in Moho depth were also documented at other stations sited within the Dharwar Craton and Southern Granulite Province of India by Rai et al. [45]. Figure 4 shows H-κ stacking results at nine typical stations obtained by adopting the approach of Zhu and Kanamori [29]. The obtained Vp/Vs and crustal thickness (H) values with error bounds for each station from the receiver functions are presented in Table 1. The estimated Vp/Vs values vary between 1.61 and 1.80. The observed large range documented in this study is nearly identical to that reported from other seismic stations sited within the Dharwar Craton and Southern Granulite Province of India (see Appendix after [45]).

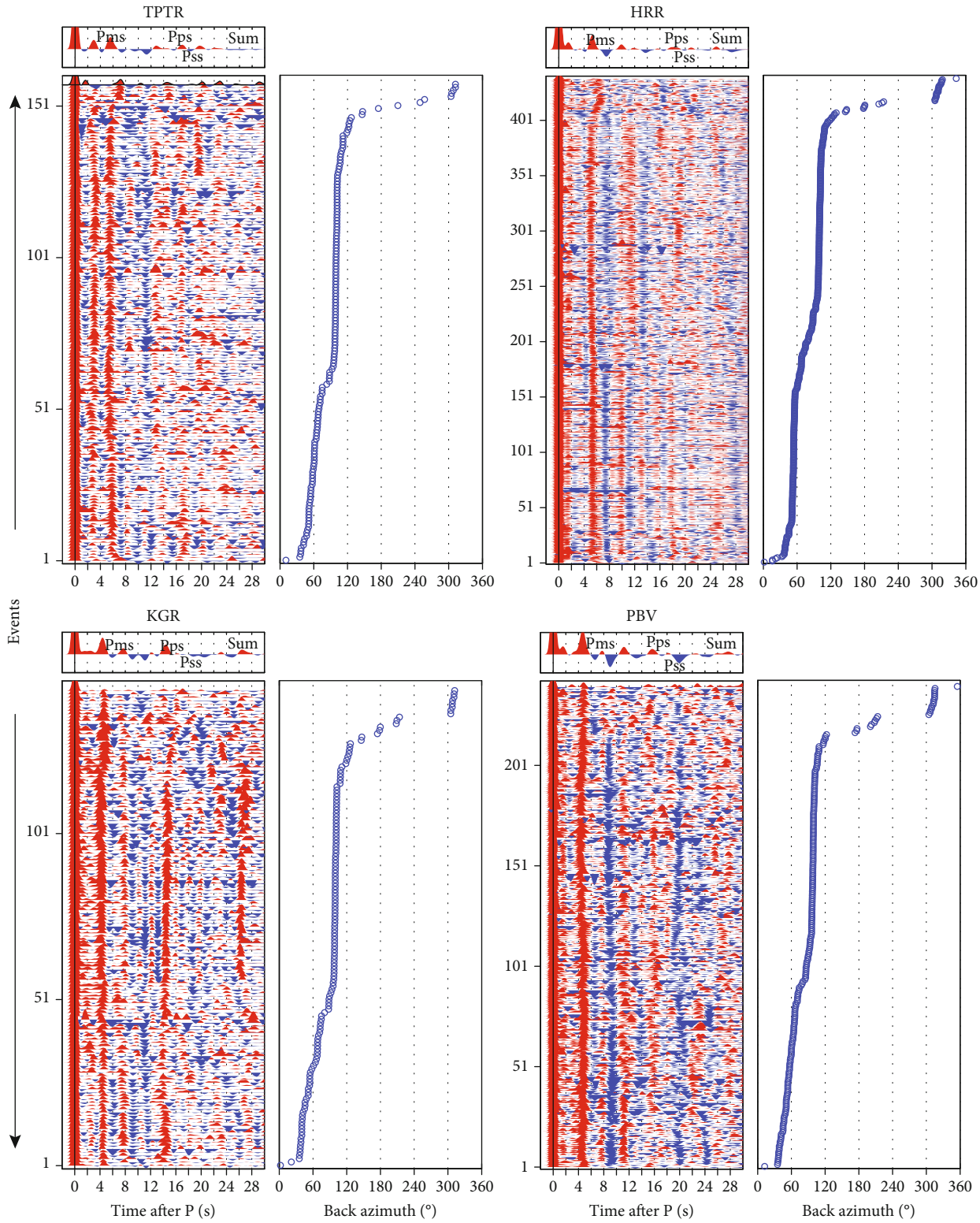

Figure 3: *P*-to-*s* (*Ps*) stacked radial receiver functions. Examples from four representative seismic stations from the Southern Granulite Province of India are shown. *Pms*, *Pps*, and *Pss* phases are marked. Each event with back-azimuth information is provided. KGR, TPTR, and HRR are sited north of MBSZ within the Eastern Dharwar Craton whereas PBV is located in Western Madurai block (Figure 1(b)).

4.2. Variation of Crustal Depth in the Study Area. The seismological results in the Southern Granulite Province of India comprise determination of Vp/Vs and crustal thickness (H) values beneath each station from recorded seismograms (see Table 1 and Figure 4). The result pertaining to Moho depth (H) is shown in Figure 5 using different-colored

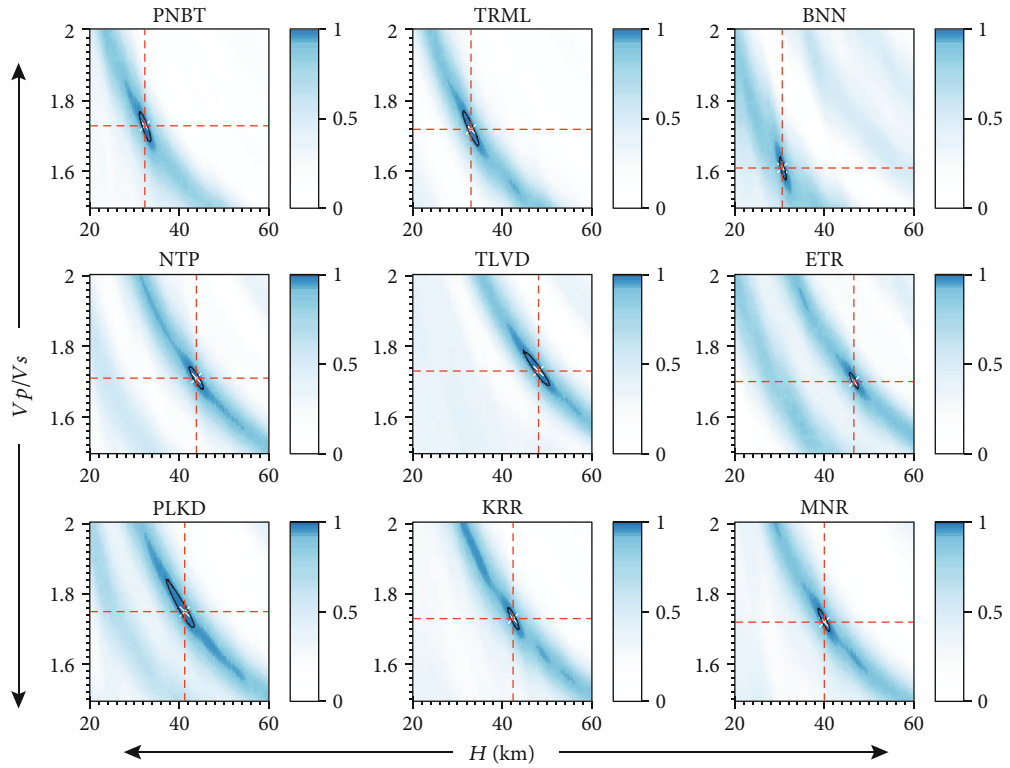

Figure 4: The H-κ stacking results for nine representative stations. These are sited (see Figure 1(b)) in Eastern Dharwar Craton (PNBT TRML, BNN, NTP, and ETR), Western Dharwar Craton (TLVD), Eastern Madurai block (KRR), and Western Madurai block (PLKD, MNR). The optimum values of H and κ are marked by point of intersection between horizontal and vertical dotted lines.

symbols. It can be noted that the crustal depth corresponding to stations sited north of Moyar–Bhavani shear zone (thick red line marked 1) is characterized by deeper Moho (>45 km). There is a major central core region bounded roughly by two thick red lines 1 and 2 (Figure 5). On the surface, line 1 approximates the Moyar–Bhavani shear zone, whereas line 2 mostly follows the Jhavadi–Karur–Kambam–Trichur boundary (thick red lines 1 and 2 in Figure 5). In this central core region, the average crustal depth (Moho) is typified mostly by uniform values ≤45 km. The Moho depth beneath the region across the meridional arm of the Jhavadi–Karur–Kambam–Trichur shear zone along the Jhavadi–Kambam arm as well as the southern arm (thick red line marked 2) varies significantly. Compared to the central core region, the Moho depth beneath stations sited in the eastern and southern segments of JKKTSZ is shallower (≤40 km) over a large area (Figure 5).

In order to obtain better insight into depth disposition of the Moho boundary across MBSZ and PCSZ (based on new data obtained from stations that were installed later), the sum traces of the receiver functions recorded at stations along four select profiles are presented (Figure 6). The profiles numbered 1 and 2 are oriented SW-NE while 3 and 4 are directed SE-NW. Three major observations that emerge from this figure are as follows: (i) large variation in the delay times of the *Pms* arrival for stations sited across MBSZ is evident in all the four profiles, (ii) the stacked sum traces reveal a clear step in depth-to-Moho on the order of 1–1.4 s (corresponding to a step of 7–10 km) across MBSZ, and (iii) the *Pms* arrivals for stations sited across PCSZ are nearly uniform, indicating no significant variation in depth-to-Moho across this shear zone (Figure 6). Concerning observation of step-in-Moho across JKKTSZ, a similar figure along 6 profiles covering the Namakkal and Madurai blocks was presented earlier ([28]). They document a clear downward step in the *Pms* arrivals ranging ~0.3–1.4 s (~2–10 km). Together, all these results reveal sudden jump (break) in Moho depth across MBSZ and JKKTSZ that constitute two of the major shear zones of the Southern Granulite Province.

4.3. CCP Stacking Results. The documented step in depth-to-Moho observed across the Moyar–Bhavani (Figure 6) and those reported earlier across Jhavadi–Karur–Kambam–Trichur shear zones are significant. Therefore in this study, in order to further comprehend the disposition of Moho depth across these two megashear zones, we transformed this information into depth domain through 2D migration and present the CCP stack images. Similarly, the CCP stack images across the Palghat–Cauvery shear zone are also obtained. The CCP stack sections along five select profiles (a–e) across MBSZ, JKKTSZ, and PCSZ are presented in Figure 7. While profile (a) cuts across the Jhavadi–Karur segment of JKKTSZ (Figure 7(a)), profile (b) traverses through two shear zones, namely, the southern arm of JKKTSZ and the PCSZ (Figure 7(b)). Two profiles (c and e) pass through both MBSZ and PCSZ (Figures 7(d) and 7(e)), and finally profile (d) transects mostly the PCSZ.

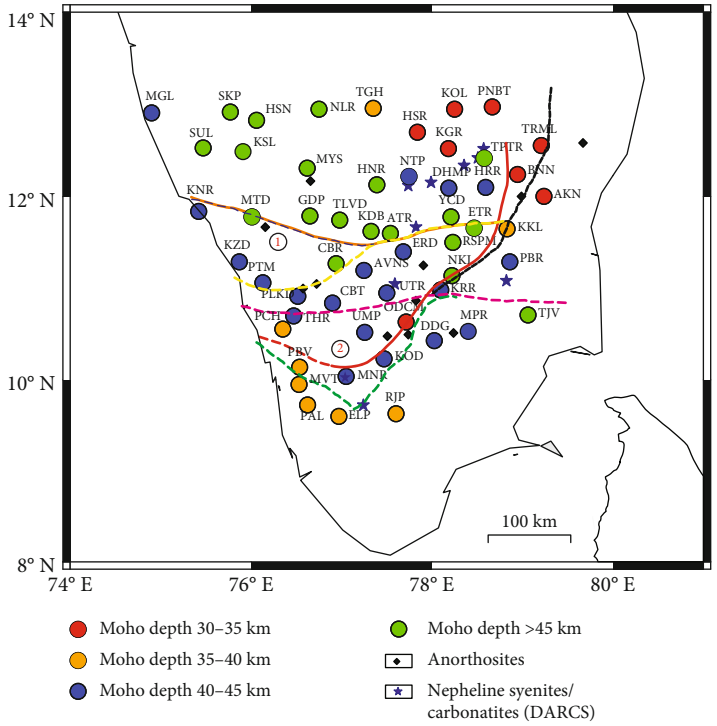

FIGURE 5: Spatial distribution of Moho depth. Three different-colored symbols are used to visualize the disposition of Moho boundary. Shear/fault zones with diverse-colored broken lines are same as in Figure 1. The distributions of alkaline rocks and carbonatites (star) and anorthosites (diamonds) are shown. Based on the distinctness in Moho depth, three regions (separated by thick red lines 1 and 2) can be demarcated as (i) region situated north of Moyar–Bhavani shear zone with deeper Moho (>45 km, green circle), (ii) a central core region with Moho depth of 40–45 km (blue circle), and (iii) a region across the meridional arm of the Karur–Kambam–Trichur shear zone up to Jhavadi with step-in-Moho depth (red/orange to blue). See text for more details.

The CCP stack images along profiles (a) and (b) across JKKTSZ document a clear step in depth-to-Moho (Figures 7(a) and 7(b)). Significantly, a prominent SE-NW dipping feature between stations HRR and KGR is distinctly observed at greater depths (Figure 7(a)). Across PCSZ, four profiles are considered (Figures 7(b)–7(e)). It can be seen that there is no noticeable variation in depth-to-Moho across PCSZ along any of these profiles. The CCP stack images across PCSZ are therefore in conformity with those observed in Figure 6 indicating a flat Moho. In this context, it may be mentioned that similar results across PCSZ are well documented independently by other researchers along multiple CCP stack profiles oriented approximately N-S (e.g., see Figure 10 of [54]). Therefore, the results of a flat Moho presented by us in Figures 6 and 7 across PCSZ of the Southern Granulite Province of India are in concert with those obtained using similar data and techniques. Finally for stations sited across MBSZ, we present CCP stack images along two profiles (Figures 7(c) and 7(e)). These images exhibit a prominent step-in-Moho depth across MBSZ and are in perfect agreement with those presented in Figure 6. Therefore, combining the results from Figures 6 and 7, a distinct step-in-Moho depth is characteristic across JKKTSZ and MBSZ, whereas no such break is apparent across PCSZ. Additionally, a SE-NW dipping feature at greater depth is also seen in the CCP stack image across JKKTSZ (Figure 7(a)) reinforcing our earlier findings of a suture.

To summarize these results in the study area, variations in depth-to-Moho in 3D are presented as Figure 8(a). This enabled us to visualize the disposition of crustal thickness across the three major shear zones of the Southern Granulite Province of India. The station locations shown in the figure provide information on the control points related to Moho depth variations. It is interesting to note that a vast region bounded by MBSZ and PCSZ, and which forms the central core region of Figure 5, is characterized mostly by uniform Moho depth extending from west to east (Figure 8(a)). This region known as the Palghat gap coincides with a geomorphic low on the surface. Therefore, the low-surface topography (Figure 1(b)) and uniform Moho depth (Figure 8(a)) over the vast area of Palghat gap are in good agreement. In this context, we would like to emphasize that there exists a strong seismological gradient (linear break) in the eastern part of PCSZ. However, this gradient should not be mistaken to have originated from suturing across the PCSZ boundary. We wish to explicitly point out that this observed linear break can be traced to the sutured SE-NW trending arm of JKKTSZ. This suture is also manifested by way of step-in-Moho depth along six profiles across JKKTSZ (see Figure 3 of [28]) which is further reinforced by the CCP stack images along two transects across the JKKTSZ (Figures 7(a) and 7(b)) in this study. Further, the three-dimensional modeling of magnetotelluric data [24] presents unprecedented insights into the subsurface electrical structure of the major shear

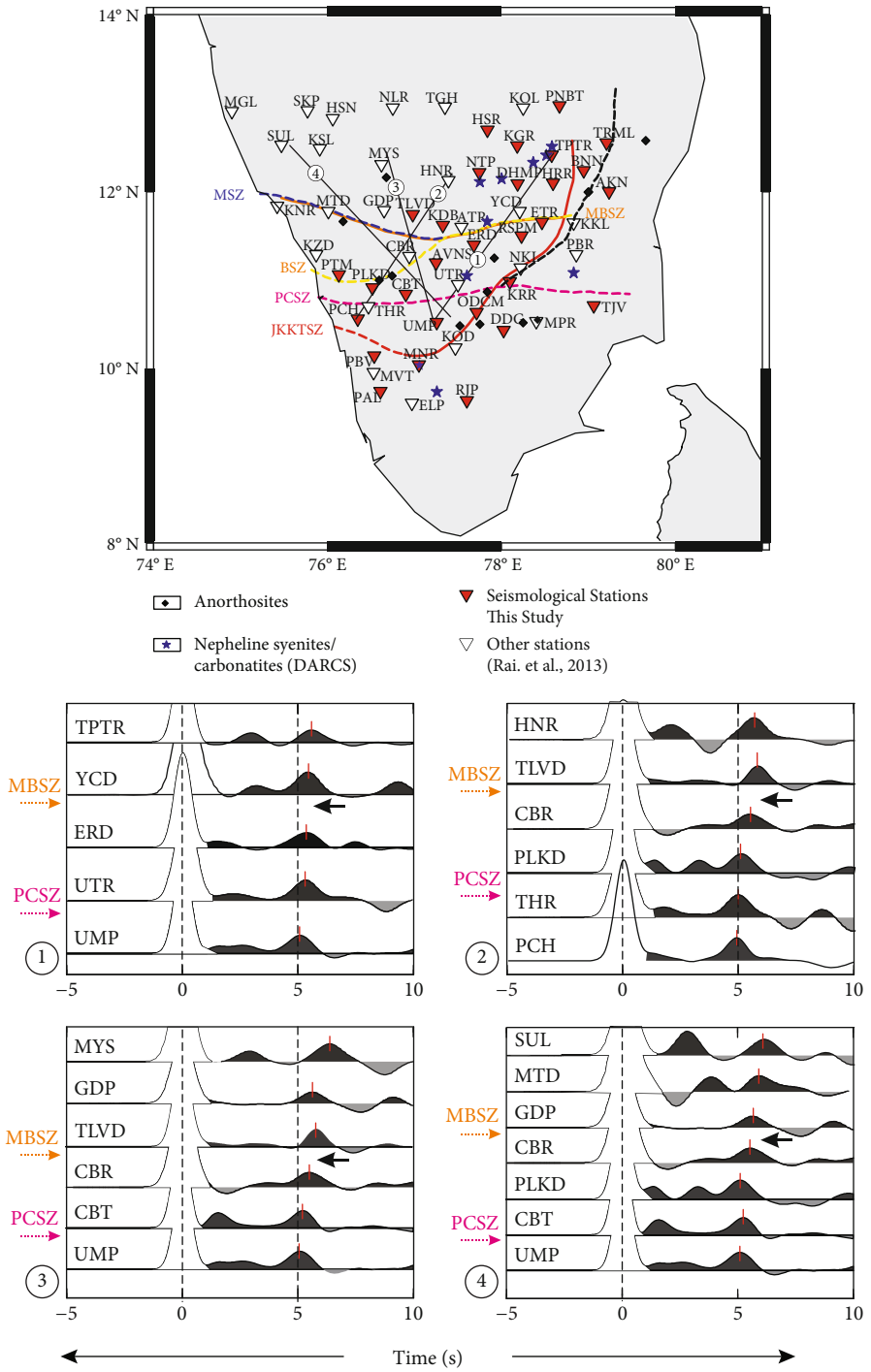

FIGURE 6: Receiver function sum traces along four profiles. These profiles (1–4) are marked in the map (top panel). Diverse-colored broken lines and thick red lines in map are same as in Figure 5. Note that each profile (1–4) traverses through PCSZ and MBSZ. Seismic station names of Rai et al. [45] are shown in italics. Consistency in *Pms* arrivals from this study and Rai et al. [45] can be noted. Location of the shear zones (bottom panel) between stations is indicated with their colored abbreviations. Black arrow indicates a clear offset in *Pms* arrivals. A step-in-Moho depth corresponding to ~7 to 10 km across MBSZ can be observed along each profile (1–4). Such offset in *Pms* arrivals is not discernible at stations sited across PCSZ. The implications of these results are discussed in the text.

zones of the Southern Granulite Province with emphasis on their depth disposition and character. A prominent conductor designated as C3 is located south of the Palghat–Cauvery shear zone. It is a major feature passing through the northern part of the Madurai block that separates the highly resistive PCSZ and Madurai block. This conductor C3 dipping southward extends from a shallow depth to much deeper levels of about 50 km into the upper mantle with a moderate

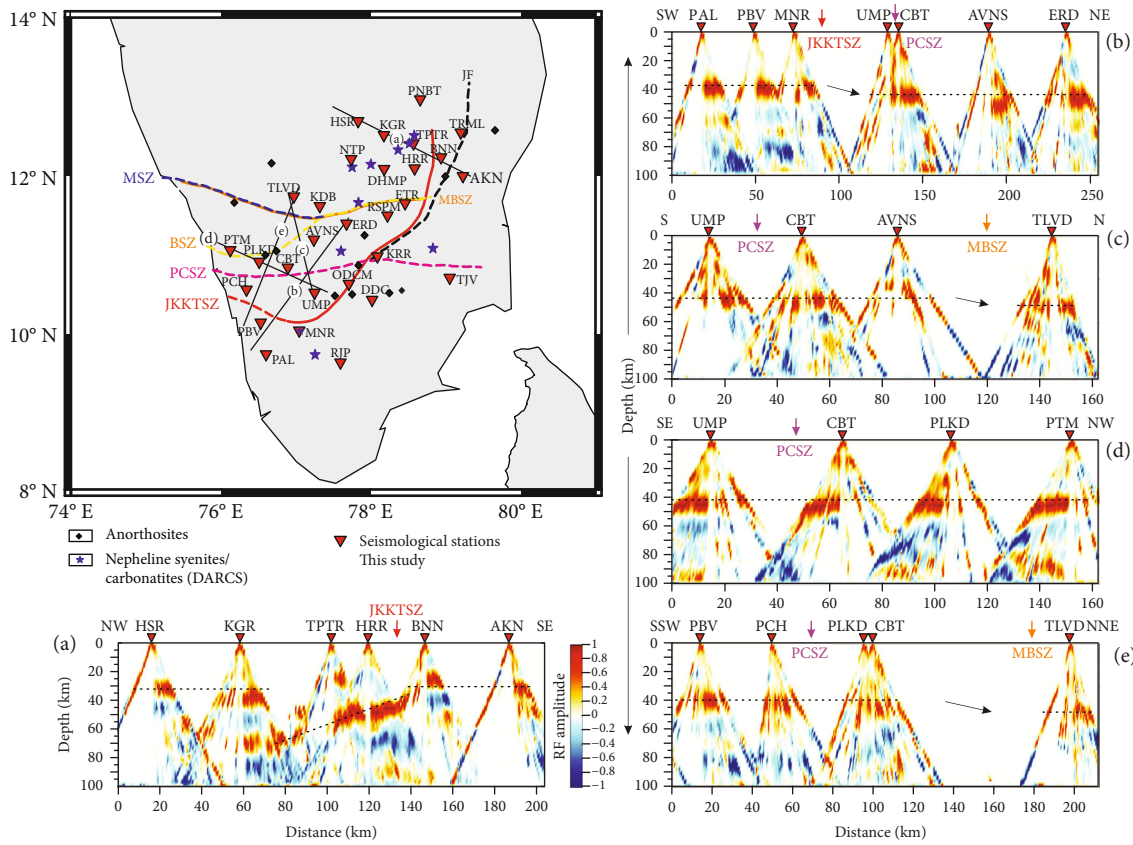

FIGURE 7: Common conversion point (CCP) stack cross-sections. Five select profiles (a–e) are marked on the map (top left panel). Diverse-colored broken lines and thick red lines in map are same as in Figure 5. Approximate Moho depth in each profile is indicated by horizontal stippled line. Clear step-in-Moho depth can be observed between stations sited across the Jhavadi–Karur–Kambam–Trichur boundary (JKKTSZ) in profiles (a) and (b). Significantly, a dipping feature at greater depth can also be seen in profile (a). Step-in-Moho at stations sited across Moyar–Bhavani shear zone (MBSZ) along two profiles (c and e) is also apparent. For stations sited across the Palghat–Cauvery shear zone, the Moho is remarkably uniform and remains flat along all the four profiles (b–e). See text for more details.

conductance of about 600 S. The close spatial correlation of this major conductor with structural feature such as the Karur–Kamban–Painavu–Trichur shear zone (KKPTSZ) assumes importance. It shows resemblance with some of the major conductive features associated with Proterozoic subduction zones [55]. Thus, it may be inferred to represent the electrical signatures of such subduction-collision zone in the Southern Granulite Province. Contrastingly, the 3D results reveal that a thick highly resistive crustal block underlies the PCSZ and a portion of the northern part of Madurai block to suggest that it is indeed a typical stable cratonic block unlike the KKPTSZ which witnessed significant reworking. These findings from 3D modeling of magnetotelluric (MT) data are consistent with our 2D-migrated seismological images that document dipping features along several profiles across the Jhavadi–Karur–Kambam–Trichur shear zone (JKKTSZ).

4.4. Composition of Average Crust of the Study Area. Utilizing the measured average crustal Vp/Vs values (data from Table 1 and Appendix) beneath each station (Figure 1(b)) and the linear relationship between SiO_2 wt% and Vp/Vs (Figure 2), we estimated the average crustal SiO_2 content in the study region. Figure 8(b) presents average crustal composition in three dimensions corresponding to the entire study area. It is interesting to note that akin to Moho depth (Figure 8(a)), the variation in average composition of the crust is apparently prominent in this diagram across the crustal-scale megashear zones.

The average silica content of the crust corresponding to stations sited north of Moyar–Bhavani shear zone is characterized by variable composition of intermediate to felsic nature (SiO_2 content centered around 62–66 wt%). In the central core region, the average SiO_2 content is typified mostly by uniform values in the range 67–68 wt%. This uniform felsic nature of the crust is therefore characteristic of the entire central core region. The average silica content across the meridional arm of the Jhavadi–Karur–Kambam–Trichur shear zone, i.e., along the Jhavadi–Kambam arm, varies significantly. While the eastern segment exhibits exceptionally high average crustal SiO_2 in excess of 70 wt% (highly felsic nature), the western counterpart is typified broadly by uniform felsic composition of 67–68 wt% (Figure 8(b)).

Based on the results presented in Figures 5–8, several inferences can be distilled:

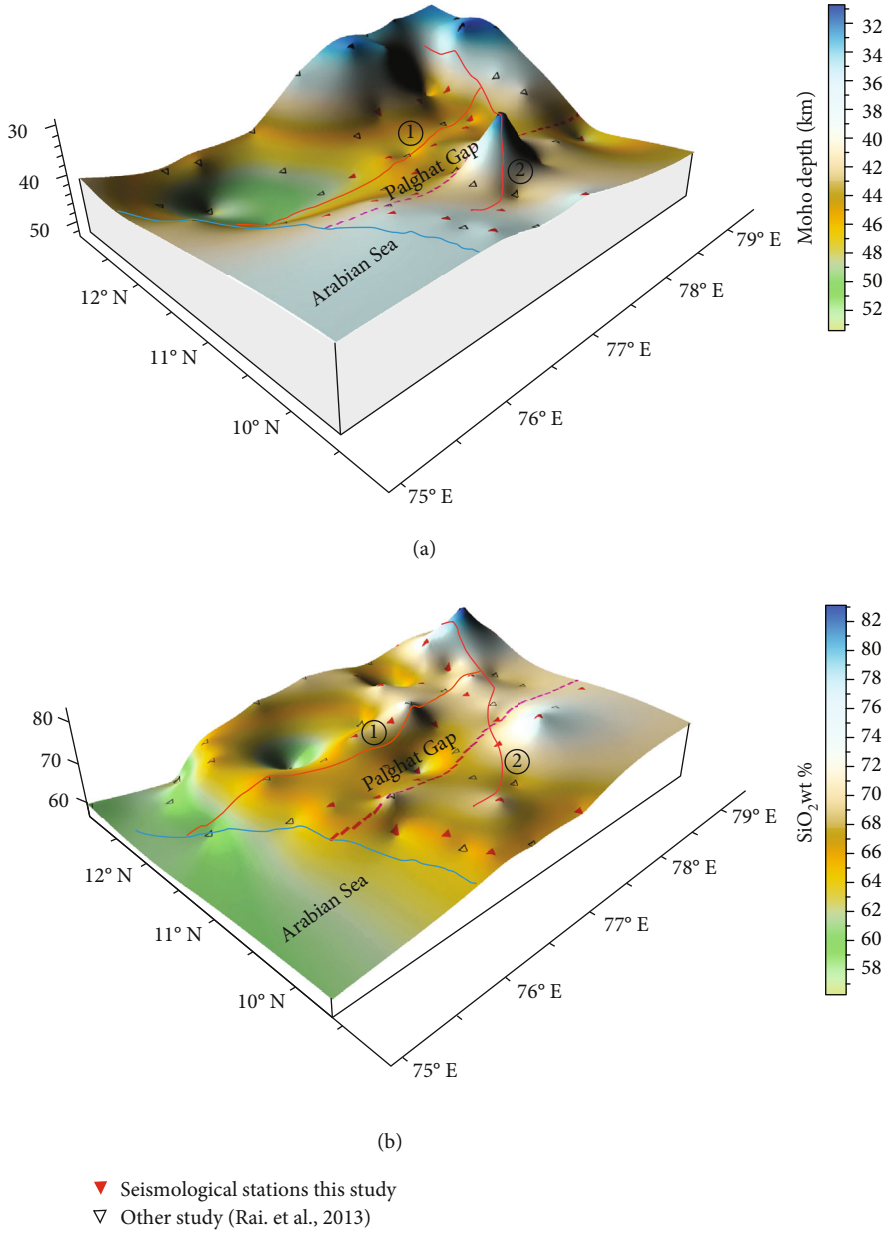

Figure 8: Three-dimensional perspective view of the crust. (a) Moho depth and (b) SiO_2 content in the studied region of the Southern Granulite Province of India. Outline of Indian continental boundary is shown by the thick blue line. Suture/shear zones with colored lines are same as in Figure 7. Note that the Moho depth and SiO_2 content vary distinctly across the two prominent shear zones, viz., MBSZ and JKKTSZ. Based on results (step-in-Moho) from individual stations, the disposition of these shear zones at Moho depth is marked by thick red lines (1 and 2). Such a feature across the Palghat–Cauvery shear zone is absent. The nature of the crust and Moho depth in the Palghat gap are largely uniform. The thick red lines (1 and 2) are inferred based on the distinctive character of the depth-to-Moho and average composition of the crust to represent two geosutures in the study region. Note their close correspondence with MBSZ and JKKTSZ on the surface. Each degree in the diagram corresponds to ~111 km. Our results demonstrate that the status of PCSZ continues to remain as a crustal-scale megashear (see text for more details). Therefore, the dashed line representing PCSZ in this figure is shown only as a reference.

(i) The thickness and average silica content of the crust beneath stations sited across the Moyar–Bhavani shear zone are distinct

(ii) A central core region representing the vast area of Palghat gap is fairly uniform in crustal characters (H-κ)

(iii) Both the Moho depth and average silica content across the Jhavadi–Karur–Kambam–Trichur shear zone vary significantly

(iv) In this context, it is important to mention that the Karur–Kambam–Painavu–Trichur shear zone at the surface was identified as a V-shaped terrane

boundary on the map by Ghosh et al. [13]. These authors demarcated the said zone based on observed lithological differences, structural studies, and geochronological data across this boundary. They attributed regional refolding to have imparted the delineated V-shaped pattern. However, several researchers do not reconcile that such a sharp feature could represent a "terrane boundary." Thus, such a peculiar disposition became contentious. Further, they do not find any field evidence to merit it as a terrane boundary (e.g., [4, 18, 32]). Based on results from the individual station locations depicting step-in-Moho, two thick red lines numbered 1 and 2 are inferred (Figures 5–8). Our results on the nature of crust (Moho depth and average SiO_2 content) clearly demonstrate that this boundary (marked as 2) at crustal depths is not so sharp. It is significant to note that the Jhavadi–Karur–Kambam–Trichur boundary at crustal depth can be viewed in the form of an arc, similar to the present-day Himalayan orogeny

(v) Furthermore, an important and interesting point worth special mention is the observation that the entire study region covering the vast area of Southern Granulite Province of India is characterized by highly felsic nature compared to the average global value of ~61.8 wt% SiO_2 reported for the continental crust ([31]; see Figure 8(b)). Although the reasons remain unclear at this stage, a focused study is warranted to explore the causal mechanism in this regard.

4.5. Comparison of Results across the Globe with Those of the Southern Granulite Province of India and Their Geodynamic Implications. At several geologic and geodynamic settings of the globe, juxtaposition of distinct crustal blocks as observed across the Moyar–Bhavani shear zone as well as the Jhavadi–Karur–Kambam–Trichur boundary in our study region is often viewed as a consequence of suturing between two geologically diverse terranes [56–63].

For example, during the period between 1.8 and 1.0 Ga, the North American Archean Craton and the Proterozoic North America got amalgamated due to suturing. Along the Abitibi–Grenville transect, results from radial receiver functions reveal abrupt variations in Moho topography on the order of 5–10 km at latitude 46.6° N close to surface expression of the Grenville Front [62]. Across the Grenville Front, a thicker crust to the south can be distinctly distinguished from thinner crust to the north. Rondenay et al. [62] ascribed the observed tapered crustal thickening followed by abrupt thinning across the Grenville Front to a suture between two colliding plates. Further, the step-in-Moho is inferred to be a relict subduction feature. The timing of collision is inferred to be Mesoproterozoic (1.71–1.23 Ga), which coincides with the timing of subduction along southeastern Laurentia [62].

Using receiver function stacked images across the Cheyenne belt, Crosswhite and Humphreys [58] recognized Proterozoic accretion (ca. 1.8 Ga old) of active arcs onto the 3.2 Ga Wyoming Craton in the central United States region. Their seismological images revealed a 100 km wide zone of 50–60 km thick crust south of the Cheyenne belt, a set of predominantly south-dipping conversions within this thick crust, and a step-in-Moho towards south near the Uncompahgre uplift. The thick crust is construed to represent a remnant from the original 1.8 Ga suturing event.

As part of the joint Lithoprobe-IRIS Canada Northwest Experiment (CANOE), Mercier et al. [61] deployed broadband seismometers in Northwestern Canada to image the crustal features associated with Wopmay Orogen. They recorded a huge jump in Moho depth (~20 km) in the radial component of receiver functions. This jump, which stretches over a horizontal distance of ~70 km on the surface, increases from ~30 km to ~50 km. The recorded anomalous jump in Moho depth is attributed to a suturing event associated with Wopmay Orogen fossil subduction during the Paleoproterozoic (1.8 Ga).

Brennan et al. [57] presented results from receiver function analyses along different transects across the central Alaska Range. They identified three distinct crustal sections based on differing crustal thickness and Vp/Vs ratios, besides the presence of intracrustal discontinuities. The documented variability in the crust across the Alaska Range was interpreted to represent amalgamation between a former continental margin and allochthonous oceanic terrane with the intermediate zone characterizing the suture zone.

Thurner et al. [63] used receiver function technique to examine the deep crustal structure in the Trans-Hudson Orogen that represents Proterozoic suturing event during 1.71–1.68 Ga between the Wyoming and Archean Superior province. The CCP stacked images exhibit evidence of massive thrusting of the Wyoming province in the west over the Superior province to the east. Besides this crustal-scale thrusting, a relic subduction feature is also documented, which is associated with the Yavapai–Superior boundary [63].

The Trans-European Suture Zone (TESZ) represents a significant lithospheric boundary in Europe that marks the transition between the Proterozoic lithosphere of the East European Craton (EEC) and the Phanerozoic lithosphere of Central and Western Europe. Using a dense network of passive seismic stations, Alinaghi et al. [56] reported results of crustal structures from (i) northern Germany to southern Sweden (TOR profile) across the Trans-European Suture Zone (TESZ). They also reported similar data from SVEKALAPKO network in Finland that gave crustal character across the Archean-Proterozoic suture. Receiver functions along the TOR profile exhibit pronounced crustal thickening north of the TESZ, besides documenting intracrustal *Ps* conversions. Likewise, data from SVEKALAPKO network indicates that towards south of the line of Archean-Proterozoic suture, a sudden deepening of the Moho by more than 20 km occurs. The receiver function data reported by Alinaghi et al. [56] could therefore confirm that sudden jump in Moho depth is characteristic of subduction zone. More importantly, in both these cases, the features associated with subduction survived through geological times despite a large difference in the geological antiquity of the regions of study (~0.9 and 1.9 Ga, respectively).

Based on P- and S-receiver function results, Knapmeyer-Endrun et al. [60] could delineate a number of tectonic subdivisions within central Europe that evolved through geologic time. These results show a sharp stepwise change in the Moho depth, on the order of 15 km (from ~30 km to more than 45 km), between the Phanerozoic Europe and the East European Craton coinciding with the Trans-European Suture Zone. The average crustal Vp/Vs ratio is also distinct across these terranes. In addition to this feature, another ancient tectonic event that took place ~1.7 Ga ago affecting the crustal configuration within Lithuania is also documented by them. For example, the crust in the eastern portion of Lithuania is on an average 5 km thicker than its western counterpart. These results have been correlated with the crustal subdivision of Lithuania along a terrane boundary of Paleoproterozoic antiquity. Distinctly different metamorphic grades, magnetic and gravimetric properties are also characteristic of the region across this terrane boundary [60]. Therefore, collectively, these results point towards a complex tectonic evolution of Europe.

He et al. [59] used H-κ stacking method to estimate the average crustal thickness (H) and the Vp/Vs ratio across the Yangtze block-Jiangnan orogenic belt-Cathaysia block in southern China. Their data revealed that the composition and seismic structure of the crust across the Jiangnan orogenic belt-Cathaysia block are identical, while these parameters are distinctly different between the two flanks of the Jiujiang–Shitai buried fault, which is delineated between the Yangtze block and Jiangnan orogenic belt. Based on these results, they proposed that the Jiujiang–Shitai buried fault defines a geosuture between the Yangtze and Cathaysia blocks.

Taking cue from all the above-mentioned studies and recognizing that distinctness in the nature of the crust induced by a past tectonic event is extensively used to delineate terrane boundaries of the geological past that survived through geological times, we prefer to interpret the results across the Moyar–Bhavani shear zone and Jhavadi–Karur–Kambam–Trichur boundary to constitute terrane boundaries (geosutures) within the Southern Granulite Province of India. The boundaries of these two sutures are marked as thick red lines (1 and 2) in Figures 5–8.

The inferences drawn from our results in the foregoing receive further support from controlled seismic source investigations carried out in the Southern Granulite Province of India [20, 64]. Seismic reflection and refraction/wide-angle reflection studies conducted along Kuppam–Palani [20] and Kolattur–Palani [64] transects of the Southern Granulite Province are reported. The Kolattur–Palani transect (Figure 1(b)) represents a segment of the Kuppam–Palani transect. This transect yielded vital information related to both MBSZ and PCSZ. Therefore, we intend to briefly highlight in the following some of their significant findings that are in good agreement with the results obtained from our receiver function analysis.

The deep seismic reflection and refraction/wide-angle reflection studies document oppositely dipping reflectivity patterns across MBSZ [20, 64], akin to subduction-related reflection fabrics at depths similar to those observed in other geographical locations worldwide (e.g., [65, 66]; see also [67] for a review). Such oppositely dipping reflectivity patterns are inferred to be signatures characteristic of collision that survived throughout the geological periods.

The velocity model of the study region points to thickening of crust across MBSZ and Dharwar Craton, which thins southward [20, 64]. This is in excellent agreement with Moho depths derived from our receiver function analysis.

The findings from 3D modeling of magnetotelluric (MT) data [24] are consistent with our 2D-migrated seismological images that document dipping features along several profiles across the Jhavadi–Karur–Kambam–Trichur shear zone (JKKTSZ), a designated terrane boundary ([28] and this study), and a flat Moho beneath the PCSZ. Together, the 3D MT and seismological results reiterate the interpretation that JKKTSZ is a candidate terrane boundary while PCSZ does not qualify as a suture.

Unfortunately, however, both the MT profiles of Patro et al. [24] terminate either south of the Moyar–Bhavani shear zone (MBSZ) or just at MBSZ. Hence, they do not provide any information about this yet another important megashear zone of SGP. Thus, related to MBSZ, we are unable to compare our findings with that of MT results.

Thus, the 3D magnetotelluric results lend unambiguous support to the seismological findings with the attendant interpretation on operation of the Wilson cycle in the Southern Granulite Province and accordingly designating some megashear zones in the study region as sutures and others as shear zones. Taken together, integration of seismic results with those obtained from other geophysical tools along the same transects point to the fact that the MBSZ and Karur–Oddanchatram shear zone (KOSZ, not shown in Figure 1 by us) could represent suture zones within the SGP [24, 64].

4.6. Geological Evidence for Terrane Boundaries and Timing of Collision across the Moyar–Bhavani and Jhavadi–Karur–Kambam–Trichur Sutures. Referring to the surface geological features, the tectonic significance on the presence of alkali syenites and related rocks that occur in the vicinity of Moyar–Bhavani and Jhavadi–Karur–Kambam–Trichur Suture Zones within the Southern Granulite Province (see Figure 1(a)) has been elaborated by Gopalakrishnan [68] and Leelanandam et al. [38]. While the former relates occurrence of alkali plutons in the region to abortive (unsuccessful) rifting, Leelanandam et al. [38] have attributed the presence of alkaline rocks and carbonatites (ARCs) and their deformed variants (DARCs) to unmistakable operation of rifting and collision processes in the region. Further, association of DARCs with ultramafic/mafic igneous bodies is also noted by them.

4.7. Moyar–Bhavani Suture. Raith et al. [17] undertook an integrated study encompassing geological, petrological, geochemical, and isotopic studies of the Nilgiri and Biligirirangan granulite terrains and the adjacent Moyar and Bhavani shear zones. Their study reveals that the Nilgiri granulite terrain represents a metasedimentary allochthonous unit. This unit has been interpreted by them to have been thrusted onto the Dharwar Craton during the Paleoproterozoic collisional

tectonics. Such an interpretation receives further support from the structural studies in key areas [69] that exhibit near-vertical movements along the Moyar shear zone with upward, northerly thrusting of the Nilgiri granulite terrain against the western Dharwar Craton. Furthermore, the presence of layered meta-anorthosite and related rock suites of Sittampundi, Bhavani, Gobichettipalayam, and other ultramafic-mafic bodies around the Moyar–Bhavani shear zone support the view that this shear zone represents a supra-subduction setting of the geological past. The Sittampundi complex is considered to be a tectonic remnant of a layered igneous body that has been recrystallized and deformed [70]. Further, the Peralimala pluton within the Moyar shear zone is an elongated body ~20 km long with an average width of about 4 km. The pluton is composed predominantly of sodic plagioclase, microcline, quartz, and hornblende with compositional variation ranging from quartz-syenite to leucogranite. In view of the possibility of Moyar shear zone representing a terrane boundary, this pluton sited within the Moyar–Bhavani Suture Zone has been interpreted to represent DARC [71]. The timing of collision of the Nilgiri block with the Archean Dharwar Craton has been estimated to be ~2.5 Ga [17]. In other words, the central block shown in Figures 5–8 collided with the Archean Dharwar Craton during 2.5 Ga forming the Moyar–Bhavani suture.

4.8. Jhavadi–Kambam–Trichur Suture. The suturing event across the Jhavadi–Kambam–Trichur took place at a later time as discussed in the following. The recent geochemical, U-Pb zircon and U-Th-Pb monazite data of Brandt et al. [22] across the Kambam–Karur arm could establish that the western domain of the Madurai province, is typically characterized by late-Neoarchean (2.53–2.46 Ga) subduction-related magnesian charno-enderbites which formed in a magmatic arc setting. The eastern part is typified by a vast supracrustal sequence that was deposited on a 1.74–1.62 Ga old basement of magnesian charnockites and hornblende-biotite gneisses. These are viewed as products of reworking of the underlying Archaean rocks. Further, it is also documented that both eastern and western domains of the Madurai province were intruded subsequently by A-type charnockites and felsic orthogneisses during 0.83–0.79 Ga. Suturing of these two domains took place giving rise to ultrahigh-temperature metamorphic rocks exposed in the area [22]. The timing of this collision event can be placed at late Neoproterozoic [22].

All these results together with multiple but independent lines of evidences (seismological, active seismic, geological, geochemical, and geochronological) when viewed collectively are significant and lend unambiguous support to the occurrence of two episodes of convergence in the study region. One took place at ~2.5 Ga between the Dharwar Craton and the central block (see Figures 5–8) along the Moyar–Bhavani Suture Zone. The second suturing event took place during the late Neoproterozoic along the Jhavadi–Karur–Kambam–Trichur region in the form of an arc, similar to the present-day Himalayan orogeny (Figures 5–8).

These inferences obviously demand an answer to another important question as to "what is the role of Palghat–Cauvery shear zone?" during the evolution of Southern Granulite Province of India. In the following, an attempt is made to address this based on the results from this study and few important field observations.

4.9. Status of Palghat–Cauvery Shear Zone. Based on the above inferences about the terrane boundaries, it is important to evaluate the status of Palghat–Cauvery shear zone, which has been argued recently to represent a terrane boundary by a number of researchers. Furthermore, this shear zone has been hypothesized to have developed as a consequence of closure of the Mozambique Ocean (e.g., [11, 72] and references therein). As pointed out above, no observable anomaly is recorded in our seismological results across this boundary. Although an in-depth review and analyses are beyond the scope of the present study, we wish to highlight some crucial points. Firstly, our seismological results (see Figures 5–8) on the nature of the crust reveal (a) flat topography of the Moho and (b) uniform average crustal SiO_2 across this shear zone. Secondly, large number of field visits ($N = 23$) conducted by us during the six-year-long operation of the broadband seismic stations provided us with ample opportunity to examine critically the Palghat gap encompassing the Palghat–Cauvery shear zone. We noticed that the Palghat gap is a ~60–70 km wide linear strip entity with an average elevation ~200 m (see Figure 1(b) for surface topography and also compare with Figure 8(a), where Moho is flat and uniform in the Palghat gap). This gap therefore represents a geomorphic low. Thus, the above two observations present an anomalous situation for the PCSZ to merit as a Proterozoic collision zone. It is important in this context to note that the collision zones in different parts of the globe are either highlands or plateaus having an altitude in excess of 600–700 m. Therefore, proponents of the idea of PCSZ as a suture need to ponder over the perplexing fact that in spite of their spatial proximity, how and why the geologically older (~2.5 Ga) Nilgiri massif could still survive its topography, while a Neoproterozoic metamorphic belt like PCSZ withered away preferentially due to erosion.

Based on our seismological results and field observations, it is unambiguously demonstrated that the Palghat–Cauvery shear zone represents only a crustal-scale megashear zone, although the causal mechanism for formation of this shear zone remains unclear at this stage. Besides the geosutures delineated in this study, there could be other fragments that might have collided with the Southern Granulite Province through geological time during its evolution. In this context, it is significant to note that a microterrane hypothesis for the Southern Granulite Province of India is already proposed [68]. Close-spaced geologic structure and geophysical crustal mapping of the entire region is therefore essential to examine this complex terrain so that further details related to its evolution could be unraveled. Special focus is warranted across the Achankovil shear zone, which could not be taken up in this study. However, it is pertinent to note that our general interpretation that large-scale thick skin tectonic disturbances have affected the SGP in the geologic past also receives unambiguous support from the presence of a well-defined north dipping conductive feature (50 to 100 Ohm m) beneath

Table 2

Station	Latitude (°N)	Longitude (°E)	Altitude (m)	No. of RF	Moho depth (km)	Vp/Vs
ATR	11.60	77.54	280	5	47.2 ± 1.90	1.69 ± 0.035
CBR	11.27	76.94	348	24	46.2 ± 0.45	1.75 ± 0.018
ELP	09.60	76.97	1114	16	38.4 ± 0.41	1.76 ± 0.012
GDP	11.79	76.65	843	16	49.3 ± 5.51	1.76 ± 0.110
HNR	12.13	77.39	594	61	45.6 ± 0.40	1.77 ± 0.009
HSN	12.83	76.06	792	20	46.1 ± 0.34	1.75 ± 0.008
KKL	11.65	78.83	155	21	38.7 ± 0.29	1.73 ± 0.020
KNR	11.84	75.42	49	20	43.5 ± 0.28	1.81 ± 0.013
KOD	10.23	77.47	2335	40	43.2 ± 0.24	1.74 ± 0.006
KOL	12.95	78.25	803	9	33.8 ± 0.47	1.74 ± 0.017
KSL	12.49	75.91	796	13	53.6 ± 2.11	1.75 ± 0.003
KZD	11.29	75.87	39	12	43.2 ± 0.55	1.77 ± 0.012
MGL	12.91	74.90	99	21	40.9 ± 0.25	1.80 ± 0.009
MPR	10.53	78.40	212	58	41.8 ± 0.24	1.69 ± 0.012
MTD	11.78	76.01	542	8	50.3 ± 0.79	1.74 ± 0.015
MVT	09.95	76.53	151	53	37.5 ± 4.31	1.76 ± 0.076
MYS	12.31	76.62	697	7	48.6 ± 4.86	1.83 ± 0.050
NKL	11.14	78.22	163	26	45.5 ± 0.48	1.71 ± 0.017
NLR	12.95	76.75	789	20	46.0 ± 5.93	1.73 ± 0.003
PBR	11.29	78.86	130	34	40.0 ± 3.68	1.73 ± 0.020
SKP	12.92	75.77	947	12	46.7 ± 0.45	1.83 ± 0.019
SUL	12.53	75.47	107	36	47.95 ± 0.14	1.81 ± 0.008
TGH	12.96	77.35	807	43	36.9 ± 0.29	1.72 ± 0.008
THR	10.7	76.47	61	7	44.45 ± 0.55	1.71 ± 0.012
UTR	10.95	77.5	267	5	44.75 ± 0.13	1.74 ± 0.012
YCD	11.78	78.21	1374	14	46.5 ± 2.69	1.73 ± 0.020

the Achankovil shear zone that forms the boundary between the Madurai and Trivandrum blocks towards farther south of our study region [24]. It is therefore interesting to note that two major features alluding to subduction-collision tectonics in the SGP, about 300–350 km apart, are delineated in the 3D models of MT. These findings are in line with the proposed microterrane hypothesis for the Southern Granulite Province of India [68].

Therefore, our seismological findings across JKKTSZ and MBSZ recognizing them as terrane boundaries receive support from field geological, petrological, and isotopic evidences. The location of two sutures at crustal depth, viz., MBSZ and JKKTSZ, is marked using thick red line based on our data from individual station locations (Figures 5–8). In the absence of seismologically discernible diagnostics and based on above cited compelling field geologic evidences with constraints from the 3D images of MT study, in the context of PCSZ, it is represented in Figure 8 as a dashed line only for purposes of reference alone.

Hence, another important outcome of this study is the inference that PCSZ represents merely a megashear zone. This shear zone is unlike the JKKTSZ and MBSZ that document seismologically delineated geosutures across them. This is a major breakthrough in our research related to Southern Granulite Province evolution. Prior to this effort, a comprehensive study of all the megashear zones of Southern Granulite Province based on judicious experimental design and integration of the apparently disparate evidences available in terms of seismic/seismological results till crustal depths, geological, geochronological, and petrological evidences reflecting the P-T processes of their deeper domains was never attempted. In our research, harnessing all these information, we arrive at a cogent model depicting the status, character, and evolution of these crustal-scale features in the context of Southern Granulite Province and place them in an appropriate geodynamic perspective.

5. Conclusions

Based on P-to-s (Ps) receiver function analyses, we presented depth images and crustal character across three prominent megashear zones of the Southern Granulite Province of India that are observed on the surface. These crustal-scale shear zones include (i) the Moyar–Bhavani shear zone, (ii) the Palghat–Cauvery shear zone, and (iii) the Karur–Kambam–Trichur shear zone. Our results yielded an unambiguous, comprehensive, and mutually consistent model of the study region. These results are capable of explaining observations

obtained from diverse specialized fields. The significant outcomes of this study are as follows:

(i) Observation of a deeper Moho (>45 km) and intermediate to felsic crust (SiO_2 = 62 – 66 wt%) to the north of Moyar–Bhavani region. The disposition of Moho boundary and average crustal composition beneath the region covering the Palghat–Cauvery shear zone (Palghat gap) is more or less uniform

(ii) Large offset in the Moho boundary and differing crustal compositions (average crustal SiO_2) are characteristic across the eastern and western segments separated by the Karur–Kambam–Trichur boundary. Such a distinction continues further northeast up to the Jhavadi on the surface

(iii) The results obtained from our receiver function analysis are in excellent agreement with those of controlled source seismic reflection and refraction/-wide-angle reflection studies conducted along the Kolattur–Palani [20, 64] transect of the Southern Granulite Province

(iv) In line with other Precambrian terranes of the globe, the nature of crust observed in our study area provides compelling evidences towards occurrence of two convergent episodes in the geological past. The first one along Moyar–Bhavani suture and the other along the Jhavadi–Karur–Kambam–Trichur suture. The geological features preserved on the surface in Moyar–Bhavani region show presence of layered meta-anorthosite, related rock suites and ultramafic-mafic bodies, typical of suprasubduction setting. In the Jhavadi–Karur–Kambam–Trichur area, the presence of *ophirags* (ophiolite fragments), alkali syenites, and carbonatites characterize the convergence

(v) Available geochronological information indicate that the first event of convergence took place during the Paleoproterozoic between the Archean Dharwar Craton and the central region (see Figures 5–8) along the Moyar–Bhavani Suture Zone. The second episode of convergence occurred later during the late Neoproterozoic period along the Jhavadi–Karur–Kambam–Trichur Suture Zone

(vi) In view of the results presented here, the current hypothesis that claims Palghat–Cauvery shear zone to have developed as a consequence of closure of the Mozambique Ocean seems flawed and totally untenable. The status of this shear zone remains only as a crustal-scale megashear

(vii) Our results assume global significance in terms of reconstruction of Gondwanaland. In that, the depth images of continental-scale megasutures discussed for the Southern Granulite Province of India can be used with certainty as the basis while evaluating similar depth images of geosutures from other fragments of Gondwanaland during supercontinent amalgamation and break-up.

Appendix

Literature data (after [45]) from 26 seismological stations that are used in the present analysis (Table 2).

Data Availability

The data presented in the current paper is available with CSIR-National Geophysical Research Institute, India and forms part of the Ph.D. thesis of the lead author, which is under evaluation. For the purposes of testing the veracity and authenticity of the data used in the current article, the data can always be made available with prior permission from the authors and institute's competent authority.

Conflicts of Interest

The authors declare that they have no conflicts of interest.

Acknowledgments

This work was carried out as part of doctoral dissertation of RP under the INDEX and MLP-6404-28 (BPK) projects sponsored by the Council of Scientific and Industrial Research, New Delhi, and CSIR-NGRI, Hyderabad. We are grateful to Sarah Roeske, Science Editor, for her useful suggestions. M. Radhakrishna, A. Singh, and two anonymous reviewers are acknowledged for critical evaluation of the manuscript.

References

[1] C. S. Pichamuthu, "Some observations on the structure, metamorphism and geological evolution of Peninsular India," *Journal of Geological Society of India*, vol. 3, pp. 106–118, 1962.

[2] P. Raase, M. Raith, D. Ackermand, and R. K. Lal, "Progressive metamorphism of mafic rocks from greenschist to granulite facies in the Dharwar Craton of South India," *Journal of Geology*, vol. 94, no. 2, pp. 261–282, 1986.

[3] B. Jayaram, "Summary of work done for the year 1904–05," *Records of Mysore Geology Department*, vol. 6, pp. 43–56, 1905.

[4] M. Ramakrishnan, "Evolution of Pandyan Mobile Belt: A Critique," in *Earth Resources and Environment*, R. Venkatachalapathy, Ed., pp. 1–40, Research Publishing, Chennai, India, 2011.

[5] Geological Survey of India (GSI) and Indian Space Research Organisation (ISRO), *Project Vasundhara: Generalised geological map: Bangalore*, Geological Survey of India, 1994, scale 1:2,000,000.

[6] L. L. Fermor, "An Attempt at the Correlation of the Ancient Schistose Formations of Peninsular India," *Memoirs of the Geological Survey of India*, vol. 70, no. 1, 1936.

[7] E. C. Hansen, R. C. Newton, and A. S. Janardhan, "Pressure, temperature and metamorphic fluids across an unbroken amphibolite facies to granulite facies transition in south Karnataka, India," in *Archean Geochemistry*, A. Kroner, A. M. Goodwin, and G. N. Hansen, Eds., pp. 161–181, Springer-Verlag, 1984.

[8] A. S. Janardhan, R. C. Newton, and J. V. Smith, "Ancient crustal metamorphism at low P_{H2O}: charnockite formation at Kabbaldurga, South India," *Nature*, vol. 278, no. 5704, pp. 511–514, 1979.

[9] R. C. Newton, J. V. Smith, and B. F. Windley, "Carbonic metamorphism, granulites and crustal growth," *Nature*, vol. 288, no. 5786, pp. 45–50, 1980.

[10] A. S. Collins and S. A. Pisarevsky, "Amalgamating eastern Gondwana: the evolution of the Circum-Indian orogens," *Earth Science Reviews*, vol. 71, no. 3-4, pp. 229–270, 2005.

[11] A. S. Collins, C. Clark, and D. Plavsa, "Peninsular India in Gondwana: The Tectonothermal Evolution of the Southern Granulite Terrain and Its Gondwanan Counterparts," *Gondwana Research*, vol. 25, no. 1, pp. 190–203, 2014.

[12] B. Meißner, P. Deters, C. Srikantappa, and H. Köhler, "Geochronological evolution of the Moyar, Bhavani and Palghat shear zones of southern India: implications for east Gondwana correlations," *Precambrian Research*, vol. 114, no. 1-2, pp. 149–175, 2002.

[13] J. G. Ghosh, M. J. de Wit, and R. E. Zartman, "Age and tectonic evolution of Neoproterozoic ductile shear zones in the Southern Granulite terrain of India, with implications for Gondwana studies," *Tectonics*, vol. 23, no. 3, article TC3006, 2004.

[14] N. B. W. Harris, M. Santosh, and P. N. Taylor, "Crustal evolution in South India: constraints from Nd isotopes," *Journal of Geology*, vol. 102, no. 2, pp. 139–150, 1994.

[15] M. Jayananda, A. S. Janardhan, P. Sivasubramanian, and J. J. Peucat, "Geochronologic and isotopic constraints on granulite formation in the Kodaikanal area, southern India," *Geological Society of India Memoir*, vol. 34, pp. 373–390, 1995.

[16] S. M. Naqvi and J. J. W. Rogers, *Precambrian of India*, Oxford University Press, New York, 1987.

[17] M. Raith, C. Srikantappa, D. Buhl, and H. Koehler, "The Nilgiri enderbites, South India: Nature and age constraints on protolith formation, high-grade metamorphism and cooling history," *Precambrian Research*, vol. 98, no. 1-2, pp. 129–150, 1999.

[18] M. Ramakrishnan, "Craton-mobile belt relations in Southern Granulite Terrain," *Geological Society of India Memoir*, vol. 50, pp. 1–24, 2003.

[19] M. Ramakrishnan, "Evolution of Pandyan mobile belt in relation to Dharwar craton [abs.]," in *International Workshop on Tectonics and Evolution of the Precambrian Southern Granulite Terrain, India, and Gondwana Correlations, Abstracts, 18–25 February 2004*, pp. 39-40, National Geophysical Research Institute, Hyderabad, India, 2004.

[20] P. R. Reddy, B. R. Prasad, V. V. Rao et al., "Deep Seismic Reflection and Refraction/Wide-Angle Reflection Studies along the Kuppam-Palani Transect in the Southern Granulite Terrain of India," in *Tectonics of Southern Granulite Terrain*, M. Ramakrishnan, Ed., vol. 50, pp. 79–106, Geological Society of India Memoir, 2003.

[21] R. M. Shackleton, "Shallow and Deep-Level Exposures of Archean Crust in India and Africa," in *The early history of the Earth*, B. F. Windley, Ed., pp. 317–322, Wiley, London, 1976.

[22] S. Brandt, M. M. Raith, V. Schenk, P. Sengupta, C. Srikantappa, and A. Gerdes, "Crustal evolution of the Southern Granulite Terrane, South India: new geochronological and geochemical data for felsic orthogneisses and granites," *Precambrian Research*, vol. 246, pp. 91–122, 2014.

[23] T. M. Mahadevan, "South Indian high-grade domain: a differentially transformed Archaean continental lithospheric segment," in *Geodynamics and Evolution of Indian Shield—Through Time and Space*, T. Radhakrishna, M. Ramakrishnan, and Narayanaswamy, Eds., vol. 74, pp. 89–99, Geological Society of India Memoir, 2008.

[24] P. K. Patro, S. V. S. Sarma, and K. Naganjaneyulu, "Three-dimensional lithospheric electrical structure of Southern Granulite terrain, India and its tectonic implications," *Journal of Geophysical Research*, vol. 119, no. 1, pp. 71–82, 2014.

[25] D. Plavsa, A. S. Collins, J. Payne, J. Foden, C. Clark, and M. Santosh, "Detrital zircons in basement metasedimentary protoliths unveil the origins of southern India," *Geological Society of America Bulletin*, vol. 126, no. 5-6, pp. 791–811, 2014.

[26] M. M. Raith, S. Brandt, P. Sengupta, J. Berndt, T. John, and C. Srikantappa, "Element mobility and behaviour of zircon during HT metasomatism of ferroan basic granulite at Ayyarmalai, South India: evidence for polyphase Neoarchaean crustal growth and multiple metamorphism in the Northeastern Madurai Province," *Journal of Petrology*, vol. 57, pp. 1729–1774, 2016.

[27] V. V. Rao, K. Sain, P. R. Reddy, and W. D. Mooney, "Crustal structure and tectonics of the northern part of the Southern Granulite terrane, India," *Earth and Planetary Science Letters*, vol. 251, no. 1-2, pp. 90–103, 2006.

[28] S. Das Sharma, R. Prathigadapa, S. Kattamanchi, and D. S. Ramesh, "Seismological mapping of a geosuture in the Southern Granulite Province of India," *Lithosphere*, vol. 7, no. 2, pp. 144–154, 2015.

[29] L. Zhu and H. Kanamori, "Moho depth variation in southern California from teleseismic receiver functions," *Journal of Geophysical Research*, vol. 105, no. B2, pp. 2969–2980, 2000.

[30] N. I. Christensen, "Poisson's ratio and crustal seismology," *Journal of Geophysical Research*, vol. 101, no. B2, pp. 3139–3156, 1996.

[31] N. I. Christensen and W. D. Mooney, "Seismic velocity structure and composition of the continental crust: a global view," *Journal of Geophysical Research*, vol. 100, no. B6, pp. 9761–9788, 1995.

[32] B. Cenki and L. M. Kriegsman, "Tectonics of the Neoproterozoic Southern Granulite Terrain, south India," *Precambrian Research*, vol. 138, no. 1-2, pp. 37–56, 2005.

[33] D. Gopalakrishna, E. C. Hansen, A. S. Janardhan, and R. C. Newton, "The southern high-grade margin of the Dharwar craton," *The Journal of Geology*, vol. 94, no. 2, pp. 247–260, 1986.

[34] J. A. Percival, J. K. Mortensen, R. A. Stern, K. D. Card, and N. J. Bégin, "Giant granulite terranes of northeastern Superior Province: the Ashuanipi complex and Minto block," *Canadian Journal of Earth Sciences*, vol. 29, no. 10, pp. 2287–2308, 1992.

[35] A. F. Wilson and T. R. Anantha, "Comparison of Some of the Geochemical Features and Tectonic Setting of Archaean and Proterozoic Granulites, with Particular Reference to Australia," in *Archaean Geochemistry*, B. F. Windley and S. M. Naqvi, Eds., pp. 241–267, Elsevier, 1978.

[36] S. A. Drury, N. B. W. Harris, R. W. Holt, G. J. Reeves-Smith, and R. T. Wightman, "Precambrian tectonics and crustal evolution in south India," *The Journal of Geology*, vol. 92, no. 1, pp. 3–20, 1984.

[37] C. R. Ravindra Kumar and T. Chacko, "Geothermobarometry of mafic granulites and metapelite from the Palghat Gap, South India: petrological evidence for isothermal uplift and rapid cooling," *Journal of Metamorphic Geology*, vol. 12, no. 4, pp. 479–492, 1994.

[38] C. Leelanandam, K. Burke, L. D. Ashwal, and S. J. Webb, "Proterozoic mountain building in Peninsular India: an analysis based primarily on alkaline rock distribution," *Geological Magazine*, vol. 143, no. 2, pp. 195–212, 2006.

[39] S. Brandt, V. Schenk, M. M. Raith, P. Appel, A. Gerdes, and C. Srikantappa, "Late Neoproterozoic P-T evolution of HP-UHT granulites from the Palni Hills (South India): new constraints from phase diagram modelling, LA-ICP-MS zircon dating and in-situ EMP monazite dating," *Journal of Petrology*, vol. 52, no. 9, pp. 1813–1856, 2011.

[40] D. Plavsa, A. S. Collins, J. F. Foden et al., "Delineating crustal domains in Peninsular India: age and chemistry of orthopyroxene-bearing felsic gneisses in the Madurai block," *Precambrian Research*, vol. 198-199, pp. 77–93, 2012.

[41] J. K. Tomson, Y. J. Bhaskar Rao, T. Vijaya Kumar, and A. K. Choudhary, "Geochemistry and neodymium model ages of Precambrian charnockites, Southern Granulite terrain, India: constraints on terrain assembly," *Precambrian Research*, vol. 227, pp. 295–315, 2013.

[42] M. Brown and M. Raith, "First evidence of ultrahigh-temperature decompression from the granulite province of southern India," *Journal of the Geological Society, London*, vol. 153, no. 6, pp. 819–822, 1996.

[43] A. Mohan and B. F. Windley, "Crustal trajectory of sapphirine-bearing granulites from Ganguvarpatti, South India: evidence for an isothermal decompression path," *Journal of Metamorphic Geology*, vol. 11, no. 6, pp. 867–878, 1993.

[44] M. Raith, S. Karmakar, and M. Brown, "Ultra-high-temperature metamorphism and multistage decompressional evolution of sapphirine granulites from the Palni Hill Ranges, southern India," *Journal of Metamorphic Geology*, vol. 15, no. 3, pp. 379–399, 1997.

[45] S. S. Rai, K. Borah, R. Das et al., "The South India Precambrian crust and shallow lithospheric mantle: initial results from the India Deep Earth Imaging Experiment (INDEX)," *Journal of Earth System Science*, vol. 122, no. 6, pp. 1435–1453, 2013.

[46] J. P. Ligorria and C. J. Ammon, "Iterative deconvolution and receiver-function estimation," *Bulletin of the Seismological Society of America*, vol. 358, pp. 233–265, 1999.

[47] K. C. Eagar and M. J. Fouch, "FuncLab: a MATLAB interactive toolbox for handling receiver function datasets," *Seismological Research Letters*, vol. 83, no. 3, pp. 596–603, 2012.

[48] R. W. Porritt and M. S. Miller, "Updates to FuncLab, a Matlab based GUI for handling receiver functions," *Computers & Geosciences*, vol. 111, pp. 260–271, 2018.

[49] K. G. Dueker and A. F. Sheehan, "Mantle discontinuity structure beneath the Colorado Rocky Mountains and High Plains," *Journal of Geophysical Research*, vol. 103, no. B4, pp. 7153–7169, 1998.

[50] S. Chevrot and R. D. van der Hilst, "The Poisson ratio of the Australian crust: geological and geophysical implications," *Earth and Planetary Science Letters*, vol. 183, no. 1-2, pp. 121–132, 2000.

[51] V. A. Egorkin, "Velocity structure, composition and discrimination of crustal provinces in the former Soviet Union," *Tectonophysics*, vol. 298, no. 4, pp. 395–404, 1998.

[52] J. Mechie, K. Abu-Ayyash, Z. Ben-Avraham et al., "Crustal shear velocity structure across the Dead Sea transform from two-dimensional modelling of DESERT project explosion seismic data," *Geophysical Journal International*, vol. 160, no. 3, pp. 910–924, 2005.

[53] I. B. Morozov, N. I. Christensen, S. B. Smithson, and L. S. Hollister, "Seismic and laboratory constraints on crustal formation in a former continental arc (ACCRETE, southeastern Alaska and western British Columbia)," *Journal of Geophysical Research: Solid Earth*, vol. 108, article 2041, 2003.

[54] M. R. Kumar, A. Singh, Y. J. B. Rao, G. Srijayanthi, H. V. Satyanarayana, and D. Sarkar, "Vestiges of Precambrian subduction in the south Indian shield? - a seismological perspective," *Tectonophysics*, vol. 740-741, pp. 27–41, 2018.

[55] A. G. Jones, "Electromagnetic images of modern and ancient subduction zones," *Tectonophysics*, vol. 219, no. 1-3, pp. 29–45, 1993.

[56] A. Alinaghi, G. Bock, R. Kind, W. Hanka, K. Wylegalla, and TOR, SVEKALAPKO, Working Groups, "Receiver function analysis of the crust and upper mantle from the North German Basin to the Archaean Baltic Shield," *Geophysical Journal International*, vol. 155, no. 2, pp. 641–652, 2003.

[57] P. R. K. Brennan, H. Gilbert, and K. D. Ridgway, "Crustal structure across the central Alaska Range: anatomy of a Mesozoic collisional zone," *Geochemistry Geophysics Geosystems*, vol. 12, no. 4, article Q04010, 2011.

[58] J. A. Crosswhite and E. D. Humphreys, "Imaging the mountainless root of the 1.8 Ga Cheyenne belt suture and clues to its tectonic stability," *Geology*, vol. 31, no. 8, pp. 669–672, 2003.

[59] C. He, S. Dong, M. Santosh, and X. Chen, "Seismic evidence for a geosuture between the Yangtze and Cathaysia Blocks, South China," *Scientific Reports*, vol. 3, no. 1, article 2200, 2013.

[60] B. Knapmeyer-Endrun, F. Kruger, and the PASSEQ Working Group, "Moho depth across the Trans-European Suture Zone from *P*- and *S*-receiver functions," *Geophysical Journal International*, vol. 197, no. 2, pp. 1048–1075, 2014.

[61] J. P. Mercier, M. G. Bostock, P. Audet, J. B. Gaherty, E. J. Garnero, and J. Revenaugh, "The teleseismic signature of fossil subduction: Northwestern Canada," *Journal of Geophysical Research*, vol. 113, no. B4, article B04308, 2008.

[62] S. Rondenay, M. G. Bostock, T. M. Hearn, D. L. White, and R. M. Ellis, "Lithospheric assembly and modification of the SE Canadian Shield: Abitibi-Grenville teleseismic experiment," *Journal of Geophysical Research*, vol. 105, no. B6, pp. 13735–13754, 2000.

[63] S. Thurner, R. Margolis, A. Levander, and F. Niu, "PdS receiver function evidence for crustal-scale thrusting, relic subduction, and mafic underplating in the Trans-Hudson Orogen and Yavapai province," *Earth and Planetary Science Letters*, vol. 426, pp. 13–22, 2015.

[64] V. V. Rao and B. R. Prasad, "Structure and evolution of the Cauvery Shear Zone system, Southern Granulite Terrain, India: evidence from deep seismic and other geophysical studies," *Gondwana Research*, vol. 10, no. 1-2, pp. 29–40, 2006.

[65] BABEL Working Group, "Evidence for early Proterozoic plate tectonics from seismic reflection profiles in the Baltic shield," *Nature*, vol. 348, pp. 34–38, 1990.

[66] S. B. Lucas, A. Green, Z. Hajnal et al., "Deep seismic profile across a Proterozoic collision zone: surprises at depth," *Nature*, vol. 363, no. 6427, pp. 339–342, 1993.

[67] W. D. Mooney and R. Meissner, "Multi-genetic origin of crustal reflectivity: a review of seismic reflection profiling of the continental lower crust and Moho," in *Continental Lower Crust*, D. M. Fountain, R. Arculus, and R. Kay, Eds., pp. 45–79, Elsevier, Amsterdam, 1992.

[68] K. Gopalakrishnan, "An overview of southern granulite terrain, India—constraints in reconstruction of Precambrian assembly of Gondwanaland," in *Tectonics of Southern Granulite Terrain*, M. Ramakrishnan, Ed., vol. 50, pp. 47–78, Geological Society of India Memoir, 2003.

[69] K. Naha and R. Srinivasan, "Nature of the Moyar and Bhavani shear zones, with a note on its implication on the tectonics of the southern Indian Precambrian shield," *Proceedings of the Indian Academy of Sciences - Earth and Planetary Sciences*, vol. 105, pp. 173–189, 1996.

[70] S. Ramadurai, M. Sankaran, T. A. Selvan, and B. F. Windley, "The stratigraphy and structure of the Sittampundi complex," *Journal of Geological Society of India*, vol. 16, pp. 409–414, 1975.

[71] K. R. Praveen, V. Prasannakumar, and M. A. Mamtani, "Time relationship between regional deformation and fabric development in the Peralimala Pluton, South India–Inferences from magnetic fabric," *Journal of Geological Society of India*, vol. 73, no. 6, pp. 803–812, 2009.

[72] A. S. Collins, C. Clark, K. Sajeev, M. Santosh, D. E. Kelsey, and M. Hand, "Passage through India: the Mozambique ocean suture, high-pressure granulites and the Palghat-Cauvery shear zone system," *Terra Nova*, vol. 19, no. 2, pp. 141–147, 2007.